2016

Raft Polymerization Of Ph-Responsive, Diblock Copolymers For Nucleic Acid Delivery Vehicles

Annie Katherine Mcclellan
University of Mississippi

RAFT POLYMERIZATION OF pH-RESPONSIVE, DIBLOCK COPOLYMERS FOR NUCLEIC ACID DELIVERY VEHICLES

A Thesis
presented in partial fulfillment of requirements
for the degree of Master of Science
in the Department of Chemical Engineering
The University of Mississippi

by

ANNIE KATHERINE MCCLELLAN

May 2016

ABSTRACT

Since the development of gene therapy, a variety of non-viral nucleic acid delivery vehicles have been prepared and studied for their transfection efficiencies. Recently, polymeric gene delivery vehicles have gained popularity for their low immunogenicity and high transfection efficiency. With the advent of controlled radical polymerization (CRP) and more specifically reversible addition-fragmentation chain transfer (RAFT) polymerization, it is now possible to develop well-defined polymers with predicted molecular weights and architectures. The work presented here focuses on the RAFT polymerization of a family of amphiphilic, cationic copolymers to be utilized for nucleic acid delivery. These copolymers are composed of a stabilizing hydrophilic block of oligo(ethylene glycol) methyl ether methacrylate (OEMGA) and a cationic, endosomolytic block of 2-(dimethylamino) ethyl methacrylate (DMAEMA), 2-(diethylamino) ethyl methacrylate (DEAEMA), or 2-(diisopropylamino) ethyl methacrylate (DPAEMA). The hydrophilic content of this copolymer series was kept constant while the degrees of polymerization of the cationic block of 25, 50, and 75 were targeted to elucidate the effects of tertiary amine functionalization on gene delivery efficacy. Means of characterization included gel permeation chromatography (GPC), dynamic light scattering (DLS), electrophoresis, and *in vitro* gene expression and toxicity studies. As a result from this study, our findings indicate the significance of cationic group functionalization on siRNA delivery, and the pH-responsive nucleic acid delivery vehicles synthesized show promise for future studies of nucleic acid delivery.

DEDICATION

I dedicate this manuscript to my loving parents, Steve and Ladye Ann McClellan, for their unending encouragement throughout my graduate studies, and my brother, Steven McClellan, for always taking care of his little sis'.

LIST OF ABBREVIATIONS AND SYMBOLS

$\bar{M}_n$	Number-average molecular weight
$\bar{M}_w$	Weight-average molecular weight
PDI	Polydispersity index
CRP	Controlled radical polymerization
NMP	Nitroxide mediated radical polymerization
ATRP	Atom-transfer radical polymerization
RAFT	Reversible addition-fragmentation chain transfer polymerization
CTA	Chain transfer agent
CSIRO	Commonwealth Scientific and Industrial Research Organization
MADIX	Macromolecular design via the interchange of xanthates
$M_{n,th}$	Theoretical number-average molecular weight
macroCTA	Macro chain transfer agent
PEI	Poly(ethyleneimine)
PEG	Poly(ethylene glycol)
DMAEMA	2-(dimethylamino) ethyl methacrylate
OEGMA	Poly(oligo(ethylene glycol) methyl ether methacrylate)
PEGMA	Poly(ethylene glycol) methyl ether methacrylate
DEAEMA	2-(diethylamino) ethyl methacrylate
BMA	Butyl methacrylate
PAA	Propylacrylic acid

DPAEMA	2-(diisopropylamino) ethyl methacrylate
GPC	Gel permeation chromatography
TAE	Tris-Acetate EDTA
DLS	Dynamic light scattering
CDP	4-cyano-4-[(dodecylsulfanylthiocarbonyl)sulfanyl] pentanoic acid
V-501	4,4’-azobis(4-cyanovaleric acid)
DMSO	Dimethyl sulfoxide
DMEM	Dulbecco’s minimal essential medium
qPCR	Quantitative polymerase chain reaction

ACKNOWLEDGEMENTS

Many people here at the University of Mississippi have supported me throughout the time I have worked on the research presented in this manuscript. I extend my gratitude to all of the faculty and staff in the Department of Chemical Engineering for supporting me throughout my graduate studies and challenging me to become the engineer I proudly call myself today. I would like to thank my advisor, Dr. Adam Smith, and fellow collaborator, Dr. Tracy Brooks, for allowing me to work in their respective research groups as well as devoting their time to serving on my thesis committee. I would also like to thank the third member of my committee, Dr. John O'Haver, for his time commitment as well as his unending encouragement throughout my tenure in graduate school. Lastly, I thank the Department of Chemical Engineering for their funding source as well as the Mississippi Space Grant Consortium for selecting me as a recipient for a research fellowship and for their funding throughout my graduate studies.

TABLE OF CONTENTS

LIST OF TABLES

LIST OF FIGURES

CHAPTER 1

POLYMERIZATION METHODS

By definition, a polymer is type of macromolecule containing a long sequence of repeating subunits; to create such molecules, a chemical synthesis or polymerization must be performed. Polymers, as a general term, can be subdivided into two broad categories, namely, naturally existing polymers such as DNA and proteins as well as synthetic polymers such as plastics, rubbers, and some pharmaceuticals.[1] Since polymers have such a wide range of uses in various industries, it is important to gain a deeper understanding of the potential characteristics and properties made possible by the numerous polymerization techniques.

1.1 Introduction to Polymers

Much like the characterization of small molecules, polymers can be categorized by their chemical composition as well as their structural arrangement. Polymers are classified as either a homopolymer or a copolymer. A homopolymer contains only a single type of repeat unit or monomer molecule. Plastics such as polyethylene and polypropylene are examples of such homopolymers. Copolymers on the other hand are made up of two or more different species or types of repeat units. Our DNA is an example of a naturally occurring copolymer while butyl rubber, as found in the inner lining of tires, is a synthetic copolymer. Copolymers can then be further subdivided by the arrangement of the different monomer species within the polymer.[1] Examples of homopolymer and copolymer arrangements can be found in Figure 1.1.

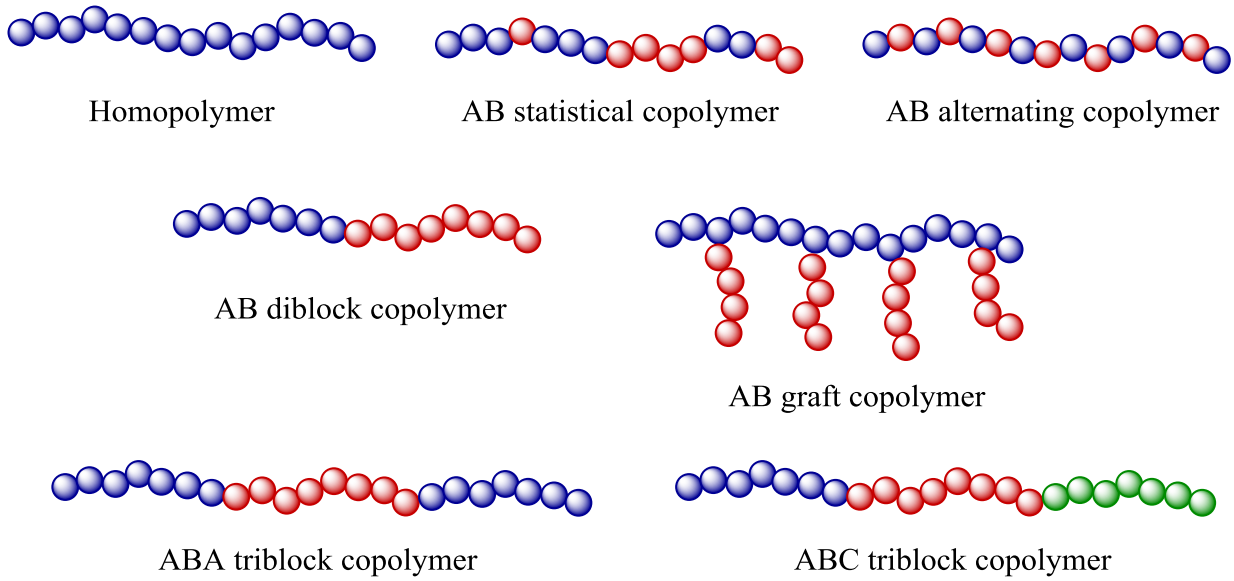

Figure 1.1 Homopolymer and copolymer architectures. Illustrated copolymer structures are AB statistical, AB alternating, AB diblock, AB graft, ABA triblock, and ABC triblock.

It is important to note that these different copolymer architectures can be used for a multitude of purposes in a variety of industries depending on the properties desired for the polymer and the application. Statistical and alternating copolymers exhibit properties that are intermediate of the corresponding homopolymers while block and graft copolymers generally exhibit full characteristics of each of the homopolymer blocks.[1] Polymers, therefore, can be synthesized with essentially any collection of physical properties depending on the monomer units and copolymer structure.

The properties of a polymer can also be affected by the size or length of the polymer chain; therefore, it is imperative to characterize the polymer dimensions by the molecular weight or the related degree of polymerization. Polymers, unlike small molecules, have a distribution of molecular weights. This distribution can be defined by either the number-average molecular weight ($\bar{M}_n$) or the weight-average molecular weight ($\bar{M}_w$) as shown in Equations 1.1 and 1.2 respectively.

$$\bar{M}_n = \Sigma X_i M_i = \frac{\Sigma N_i M_i}{\Sigma N_i} \quad \text{(Eq. 1.1)}$$

$$\bar{M}_w = \Sigma w_i M_i = \frac{\Sigma N_i M_i^2}{\Sigma N_i M_i} \quad \text{(Eq. 1.2)}$$

As defined in Equation 1.1, the number-average molar mass is the sum of the products of a molecule's molar mass (M_i), and the mole fraction (X_i) of that particular molar mass in the polymer sample. Similarly as defined in Equation 1.2, the weight-average molecular weight is the sum of the molecules with weight fraction (w_i) in the polymer multiplied by the molar mass of the molecules in this weight fraction. The ratio of these two values, $\bar{M}_w/\bar{M}_n$, is known as the polydispersity index (PDI) which indicates the width of the molar mass distribution and gives insight into the range of molecular weights of a given polymer. Should the PDI near unity, the polymer would be considered monodisperse meaning that all of the polymers are of roughly the same length and molecular weight.[1] To quantify the number of repeat units of a given species with the polymer structure, the degree of polymerization is calculated by dividing the molecular weight of the polymer by the repeat unit molecular weight as shown in Equation 1.3.

$$\bar{x}_n = \frac{\bar{M}_n}{M_0} \quad \text{(Eq. 1.3)}$$

1.2 Polymerization Principles

To create a polymer, as briefly mentioned, a series of reactions must occur to chemically link a number of monomer units together. For this process to be possible, the monomer molecules must have a functionality of two or more. In other words, the monomer must be capable of reacting with at least two other monomers so to form a link of monomer units which ultimately leads to the formation of a polymer. Considering that there are many varieties of chemical reactions and

polymerization methods with even more monomer molecules available, it is best to categorize polymerization reactions into two categories: step-growth polymerization and chain-growth polymerization.[1] A generalized schematic for both of these polymerization methods is illustrated in Table 1.1.

Table 1.1 Schematic for step-growth and chain-growth polymerizations (o: monomer repeat unit, I: initiator species).

	Step-Growth	Chain-Growth
Dimer	o + o → o-o	I + o → I-o I-o + o → I-o-o
Trimer	o-o + o → o-o-o	I-o-o + o → I-o-o-o
Tetramer	o-o-o + o → o-o-o-o o-o + o-o → o-o-o-o	I-o-o-o + o → I-o-o-o-o
Pentamer	o-o-o-o + o → o-o-o-o-o o-o-o + o-o → o-o-o-o-o	I-o-o-o-o + o → I-o-o-o-o-o

For step growth polymerizations, reactions can occur between any two molecular species in the polymerization solution in order to grow the polymer chains. Though monomer molecules are consumed quickly during the early phases of the polymerization, the degree of polymerization increases throughout the reaction since two polymer chains can join to form one much larger polymer chain. One negative aspect of this polymerization method though is that it is not ideal for synthesizing large molecular weight polymers. Since the monomers are consumed early in the reaction, only polymer chains are available to move around in solution and react with each other to form the larger polymer chains. Even moderately long polymer chains do not move well in solution since steric hindrance affects the range of motion and molecular diffusion. This loss of mobility means large molecular weight polymers are more difficult to synthesize by step growth polymerization.[1]

On the other hand in chain-growth polymerizations, monomer molecules are consumed throughout the entire polymerization reaction, and larger molecular weight polymers with high degrees of polymerization are possible. Once polymerization has been initiated, the chain growth occurs very rapidly with successive additions of monomer molecules to the growing polymer chain. When the polymer chain becomes terminated, it is no longer able to propagate, and the overall degree of polymerization does not change; however, the number of polymer chains formed increases.[1]

1.3 Radical Polymerization

Radical polymerizations, one type of chain grown polymerization, are the most widely used polymerization method to date and are known for their versatility to utilize a wide range of unsaturated monomers. The polymer grows by the reaction between an unsaturated molecule and a molecule containing a free radical as shown in Scheme 1.1. Being a type of chain growth polymerization, propagation during a radical polymerization occurs by the sequential additions of monomer units to the radical reactive site otherwise known as the active center. For all radical polymerizations, the free radical on the end of the chain attacks a monomer causing homolytic cleavage of the π-bond. One electron from this broken π-bond forms a new covalent bond between the two molecules, and the lone, free electron then moves to the terminal carbon atom creating a new active center.[1]

Scheme 1.1 Radical polymerization mechanism. The polymer growth is indicated by sequential addition of an unsaturated molecule to the active center to create a new active center.

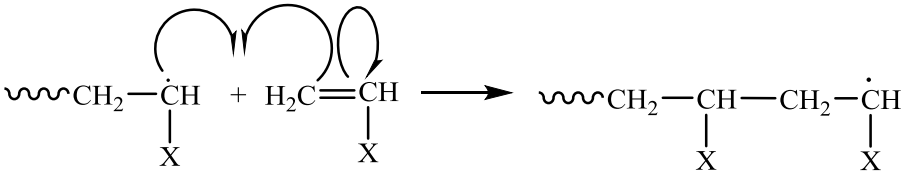

Radical polymerizations can be further divided into two main categories: conventional free radical polymerization and controlled radical polymerization (CRP). These two categories mainly differ by the amount of time that the free, active radicals are present during the polymerization process. For free radical polymerizations, the radical sites are active for most of the time during the polymerization; however, for CRP, the radical sites are only active for short bursts of time. The CRP techniques afford better control over the resulting polymers as much research has been completed in this area since their development in the 1990s.[1]

1.4 Controlled Radical Polymerization

For reversible-deactivation polymerizations the radical sites are only active for a short amount of time since they are temporarily deactivated throughout the polymerization by being reversibly trapped by another molecular species. The CRP techniques, utilizing the reversible-deactivation strategy, work to limit termination events resulting in the polymerization techniques maintaining most of the active sites throughout the polymerization. If all of the polymer chains can be initiated at the same time, the end result yields a polymer with a PDI close to one.[1] This living quality of the CRP methods makes them very valuable in a number of industries such as pharmaceutics.[2-4]

There are two documented mechanisms to gain the pseudo-living quality of the CRP methods. The first strategy involves a reversible end-capping process as shown in Figure 1.2a. Here, a chain-capping species (denoted R) reversible reacts with a propagating radical chain. The polymer can only grow when species R is not bound to the radical chain, and it ceases propagation when the chain-capping species is bound. The second CRP strategy utilizes a degenerative chain transfer mechanism as illustrated in Figure 1.2b. This strategy relies on a chain transfer reaction in

which a free radical chain displaces the non-radical chain causing a transfer of the active species from one chain to another. Both the reversible end-capping and degenerative chain transfer strategies must include a rapid, reversible exchange of the active species to ensure that each polymer chain grows with the same probability. Also, due to the temporary deactivation of radical species throughout the polymerization that results in low radical concentrations, termination events for both strategies are almost completely suppressed[1].

(a) Reversible end-capping

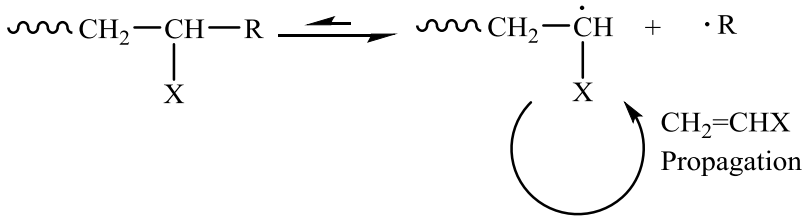

(b) Degenerative chain transfer

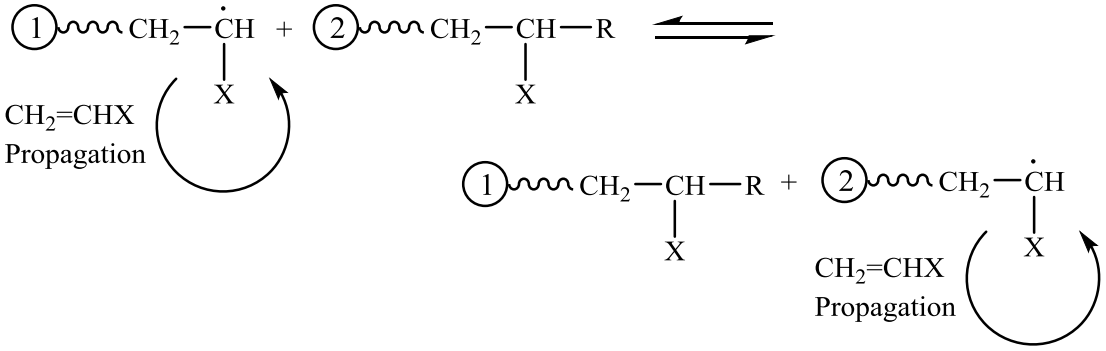

Figure 1.2 Controlled radical polymerization strategies: (a) reversible end-capping method and (b) the degenerative chain-transfer strategy.

There are three main types of CRP methods: nitroxide mediated radical polymerization (NMP), atom transfer radical polymerization (ATRP), and reversible addition-fragmentation chain transfer (RAFT) radical polymerization. Both NMP and ATRP utilize the reversible end-capping strategy while RAFT utilizes the degenerative chain-transfer mechanism. Briefly, NMP employs nitroxide radicals as the end-capping group while ATRP utilizes a transition metal-halide

complex.[1] RAFT, on the other hand, utilizes a chain transfer agent (CTA) to mediate the degenerative chain transfer process.[1-2, 5-6]

1.5 RAFT Polymerization

Reversible addition-fragmentation chain transfer (RAFT) polymerization was first reported in 1998 by the Commonwealth Scientific and Industrial Research Organization (CSIRO) in Australia.[5-6] Independently, a French research group led by Bouhadir patented the same process under the name Macromolecular Design via the Interchange of Xanthates (MADIX).[8-9] Though the names differ, both polymerization methods are dependent on a degenerative chain transfer process utilizing a controlling agent for polymer synthesis. Since its invention, RAFT has become one of the most widely used polymerization methods because of the variety of tolerable functional monomers available and because it creates near monodisperse polymers of well-defined molecular weight and architecture.[2]

1.5.1 RAFT Mechanism

The RAFT polymerization mechanism, as illustrated in Scheme 1.2, utilizes a thiocarbonylthio CTA to support the living polymerization characteristics associated with the controlled radical polymerization methods. The main stages of RAFT polymerization are the initiation or generation of radicals, activation of the CTA, propagation of polymers, and termination of the polymer chains.[1-2, 10]

To initiate RAFT polymerizations, primary radicals must be generated as with any traditional radical polymerization method (Scheme 1.2; Reaction 1); therefore, initiation processes utilizing energy sources such as heat, UV radiation, or gamma radiation may be employed.

Contrary to conventional radical polymerization methods, the primary radical species react with and activate the RAFT chain transfer agent.[1-2, 10] Some common thermal initiators are shown in Figure 1.3. [4, 10]

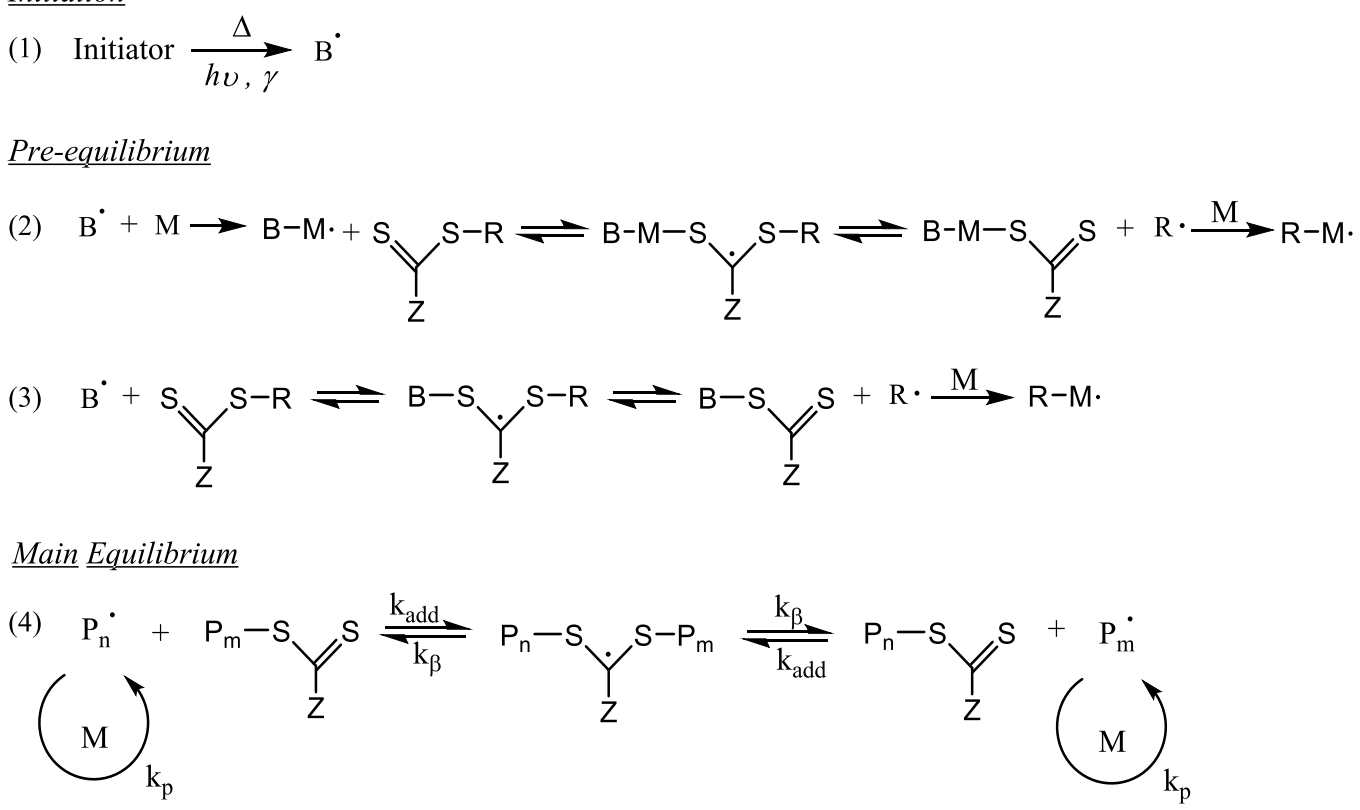

Scheme 1.2 RAFT polymerization mechanism. Reaction steps include (1) radical initiation of the initiator species utilizing heat or radiation, (2, 3) CTA activation by a radical species and pre-equilibrium with formation of oligomers, (4) main equilibrium of the RAFT polymerization with propagating polymer chains, and (5) termination of polymer chains.

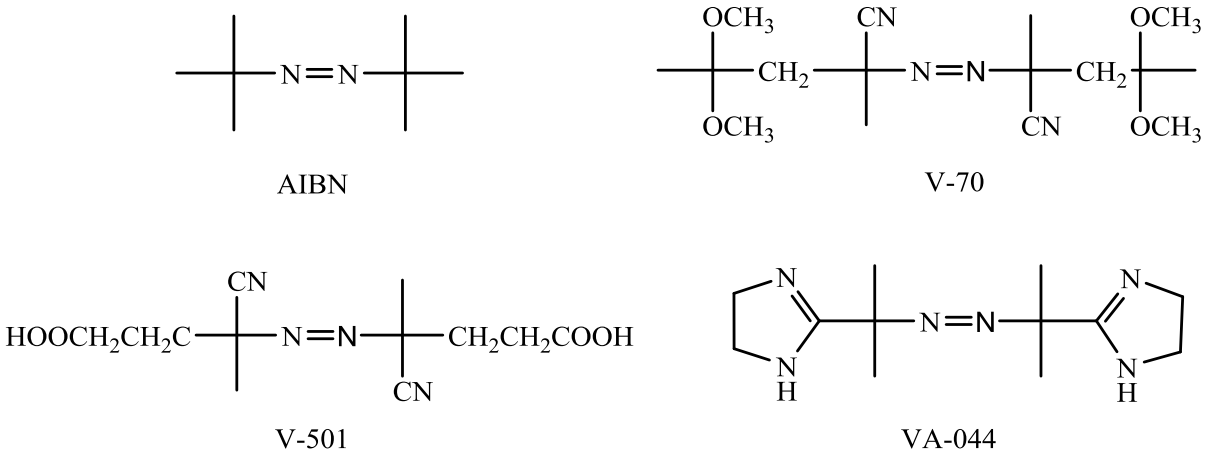

Figure 1.3 Common thermal initiators.

Once there are radical species in solution, the activation of the RAFT agent can occur by one of two different mechanisms (Scheme 1.2, Reactions 2 and 3). Since the monomer concentration is much larger than the CTA concentration, the primary radical has a higher probability of activating a monomer molecule over a RAFT agent (Scheme 1.2, Reaction 2). The activated monomer species can then react with either other monomer units or the RAFT agent. Considering the high chain transfer constant of the CTA, it is unlikely that many monomers will react with the activated monomer before reacting with a CTA. Once the CTA has been activated forming the intermediate species, the fragmentation process occurs when the leaving group homolytically cleaves and is now able to react with monomers in solution. In order to ensure this R group fragmentation, it is advantageous to choose a CTA in which the R group is a better free radical leaving group than the activated monomer. Alternatively, the primary radical may directly react with the CTA forming the intermediate radical (Scheme 1.2, Reaction 3). Again, the fragmentation process occurs, and the leaving R group can now propagate in solution by reacting with monomer molecules.[1-2, 10]

It is important at this time to note the ratios of the polymerization mixture in order to make the kinetics of this pre-equilibrium step, as well as the overall RAFT mechanism, more apparent. Ideally, there will be a CTA to initiator ratio ranging from 2:1 to 10:1. The CTA controls the number of polymer chains while the initiator dictates the number of free radicals in the system. Since the initial initiator concentration is much less than the initial CTA concentration, there will be more dormant polymers in the system than activated polymer chains. The pre-equilibrium stage encompasses the activation of the RAFT agents and the beginning of polymer formation in which only oligomers are formed.[2, 10] After all of the CTAs have been activated, the polymerization moves into the main equilibrium stage in which the bulk of the monomer molecules are consumed. It is this point in the polymerization that the living characteristics become apparent (Scheme 1.2, Reaction 4). Here, the CTAs undergo the degenerative chain transfer process between polymer chains with only the radical species propagating in solution while the thiocarbonylthio species remains dormant.[1-2]

For termination of the polymerization to occur, a few situations are possible. The reaction can go to completion to the point where there are no more monomer molecules in solution able to react with propagating polymer chains. The reaction mixture can also be introduced to an atmosphere containing a high concentration of radical species such as oxygen. Bimolecular reactions in which two radical chains undergo a combination or disproportionation termination process ultimately leading to a dead polymer are also possible. Once the polymer chains are inactive from a termination process, they can no longer propagate and the polymerization is complete.[10]

1.5.2 RAFT Chain Transfer Agent (CTA)

The chain transfer agent is imperative to the RAFT polymerization process in order to successfully achieve the desired living conditions; therefore, the CTA must be carefully chosen for each RAFT polymerization. A wide variety of thiocarbonylthio RAFT agents with the general structure RSC(=S)Z have been identified and reported in the literature. Figure 1.4 illustrates the four subcategories of the thiocarbonylthio structural family including dithioesters, xanthates, dithiocarbamates, and trithiocarbonates. An effective RAFT agent must have a reactive carbon-sulfur double bond (C=S) and result in a radical that can reinitiate the polymerization process. The CTA must also give an intermediate radical that favors the elimination of the free radical leaving group. Some commonly used RAFT agents are illustrated in Figure 1.5. [2, 4, 10]

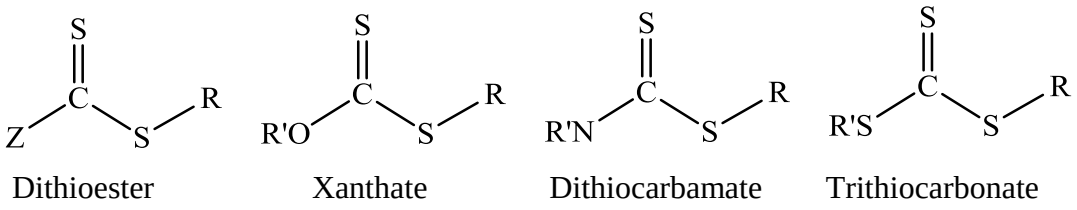

Figure 1.4 General structure of the RAFT chain transfer agents.

When choosing a CTA for the desired polymerization, it is imperative to recognize how the CTA will interact with the monomer and resulting polymer chains. These interactions are what ultimately affecting the RAFT polymerization kinetics.[4, 10] Figure 1.6 illustrates the structures of a dithioester RAFT agent throughout the polymerization process.[2] Compound (1) includes the reactive C=S double bond as well as a Z group capable of activating this double bond.[10-11] The intermediate radical illustrated by compound (2) includes two free radical leaving groups, R and R'. For this CTA to be effective, the R group must contain a weaker single bond capable of fragmenting from the CTA intermediate. Also, the Z group ensures stabilization for the duration

of the equilibrium. Finally, once the R group has fragmented and is a free radical in solution, it must be capable of reinitiating polymerization. Then the addition-fragmentation chain transfer mechanism occurs in the opposite direction to develop a new propagating radical thus moving the polymerization process into the main equilibrium.[2, 10]

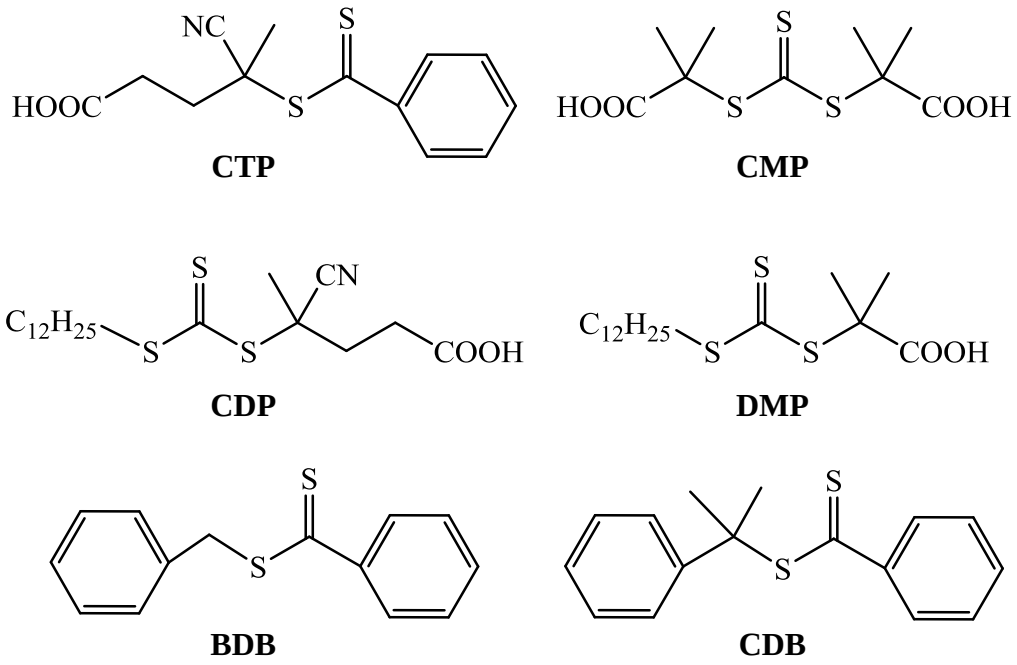

Figure 1.5 Commonly used chain transfer agents in RAFT polymerization.

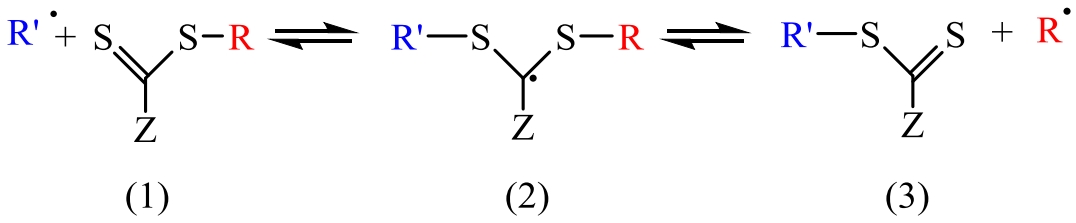

Figure 1.6 CTA structures during RAFT polymerization

1.5.3 Molecular Weight Control

RAFT polymerization is well known for its control over the polymer molecular weight. The innate living conditions provided by the RAFT agent in part allows for this regulation over

the molecular weight; however, there are other conditions that must be met to afford the desired control. The two main sources of polymer chains during the RAFT polymerization process are the radical initiator fragments formed from homolytic cleavage of the initiator as well as the radical CTA leaving groups formed from the CTA fragmentation step. Taking these radical sources into consideration, the equation for the theoretical number-average molecular weight ($M_{n,th}$) from a RAFT polymerization is given in Equation 1.4.

$$M_{n,th} = \frac{[M]_0 M_{MW} \rho}{[CTA]_0 + 2f[I]_0(1-e^{k_d t})} + CTA_{MW} \qquad \text{Eq. 1.4}$$

$[M]_0$	initial monomer concentration
M_{MW}	monomer molecular weight
ρ	monomer conversion
$[CTA]_0$	initial CTA concentration
f	initiator efficiency
$[I]_0$	initial initiator concentration
k_d	initiator decomposition rate constant
CTA_{MW}	CTA molecular weight

From the denominator of Equation 1.4, it can be determined that the CTA to initiator concentration plays a role in the control of the polymer molecular weight. Should the ratio of $[CTA]_0$:$[I]_0$ be sufficiently high, the fraction of polymer chains initiated from radical initiator fragments will be less than 5% of the overall polymer chain sources[7]; therefore, the initiator term in the denominator can typically be ignored, and Equation 1.4 can be simplified to Equation 1.5.

$$M_{n,th} = \frac{[M]_0 M_{MW} \rho}{[CTA]_0} + CTA_{MW} \qquad \text{Eq. 1.5}$$

This equation now clearly indicates a linear relationship between polymer number-average molecular weight and monomer conversion (ρ); therefore, after analysis of experimental kinetic

data of the desired RAFT polymerization, polymers of a predetermined molecular weights and narrow polydispersity can be produced.[10]

1.5.4 Block Copolymer Synthesis

Block copolymers have a wide range of applications since they express characteristics of the homopolymer components as well as properties resulting from homopolymer linking. RAFT polymerization is a powerful method for the development of complex polymer architectures, and it is commonly employed for the synthesis of block copolymers.[1-2] Polymers synthesized via RAFT polymerization contain a thiocarbonylthio end group in the polymer structure. This polymer, now termed the macro chain transfer agent (macroCTA), reacts similarly to the low molecular weight CTA utilized for developing homopolymers, and it can be chain extended with another monomer species to form the desired AB diblock copolymer.[2] The generalized RAFT synthesis of diblock copolymers is illustrated in Figure 1.7.

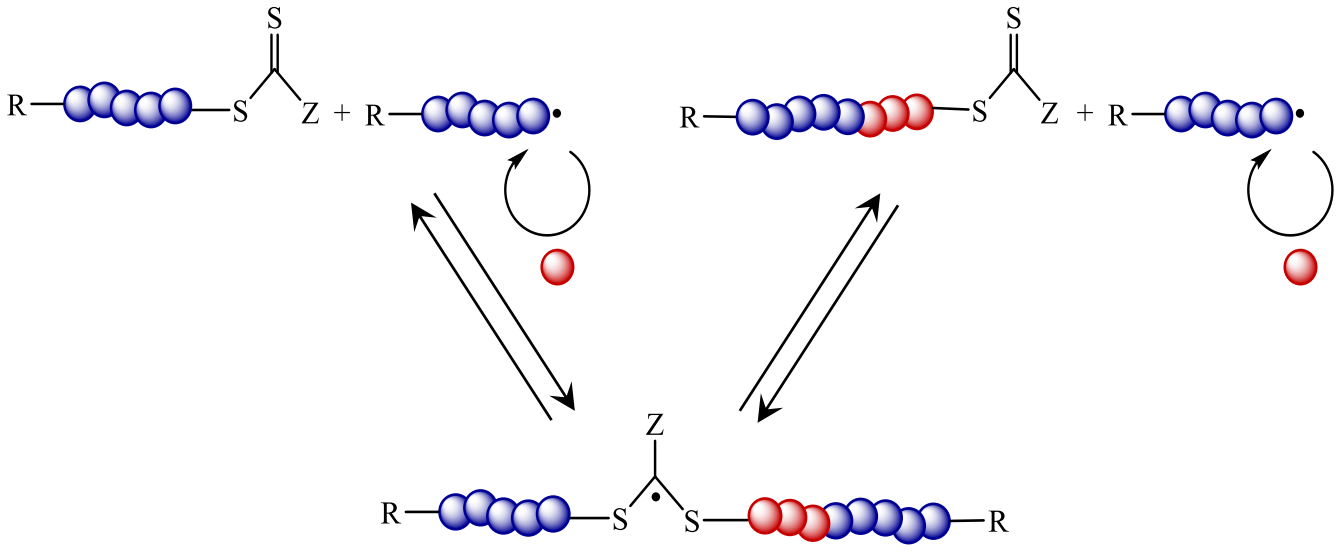

Figure 1.7 General mechanism for the RAFT synthesis of diblock copolymers

Much like homopolymer synthesis, after initiation the propagating polymer chain will undergo addition to the macroCTA by attacking the π-bond of the thiocarbonylthio end group. The originally dormant polymer will then preferentially fragment from the intermediate species resulting in a new active polymer capable of chain extending with the second monomer species. The originally active polymer is now dormant with the thiocarbonylthio end group.[1-2]

Polymer sources during diblock copolymer synthesis originate from the radical initiator fragments from the original initiation step and the polymer radicals that have fragmented from the macroCTA intermediate compound. Knowing these polymer chain sources, the block copolymer molecular weight can be calculated similarly to that of a homopolymer as denoted in Equation 1.6 with the percentage of dead polymer chains defined in Equation 1.7.[2]

$$M_{\text{block copolymer}} = \frac{[M]_0 M_{MW} \rho}{[\text{macroCTA}]_0 + 2f[I]_0(1-e^{k_d t})} + M_{\text{macroCTA}} \qquad \text{(Eq. 1.6)}$$

$[M]_0$	initial monomer concentration
M_{MW}	monomer molecular weight
ρ	monomer conversion
$[\text{macroCTA}]_0$	initial macroCTA concentration
f	initiator efficiency
$[I]_0$	initial initiator concentration
k_d	initiator decomposition rate constant
M_{macroCTA}	macroCTA molecular weight

$$\%_{\text{ dead chains}} = \frac{2f[I]_0(1-e^{k_d t})}{[\text{macroCTA}]_0 + 2f[I]_0(1-e^{k_d t})} \qquad \text{(Eq. 1.7)}$$

It can be inferred that a high $[\text{macroCTA}]_0$:$[I]_0$ ratio indicates that the majority of the polymer chains are generated from the macroCTA; therefore, the molecular weight calculation for a block copolymer can be simplified to Equation 1.8 by neglecting the initiator terms. A linear

relationship between block copolymer molecular weight and monomer conversion can now be observed, and the polymerization kinetics can be somewhat predicted to produce polymers of well-defined molecular weight and architecture. The high $[\text{macroCTA}]_0$:$[\text{I}]_0$ ratio also indicates an inverse relationship between dead polymer chains and initial macroCTA concentration; therefore, having a higher concentration of macroCTA in the polymerization solution would cause most of the polymer chains to remain in the main equilibrium stage of RAFT polymerization resulting in a polymer of low molecular weight dispersity.

$$\text{M}_{\text{block copolymer}} = \frac{[M]_0 M_{MW} \rho}{[\text{macroCTA}]_0} + \text{M}_{\text{macroCTA}} \qquad \text{(Eq. 1.8)}$$

CHAPTER 2

GENE DELIVERY

Gene therapy is a novel approach to replacing or modifying the use of drugs or other therapies that treat symptoms in patients.[12] This therapeutic method utilizes a gene delivery vehicle to transport genetic material into affected cells in order to alter expression of existing genes, supplement existing proteins, or induce cytotoxic activity. Though the first gene therapy trials began in 1990, it wasn't until the year 2000 that the first successful gene therapy treatment was reported. With this success came an increased interest in the development of gene therapies, lending to the pursuit of a safe and effective gene delivery vehicle for clinical use.[13]

Both viral and non-viral gene delivery vehicles have been studied and characterized for their gene delivery efficiencies. The production of non-viral vehicles has gained much more attention, however, since viral vectors tend to induce an immunogenic response and are considered toxic to cells.[14-15] The two categories of non-viral vehicles studied are natural polymers such as chains of amino acids and synthetic polymers (usually cationic) with the majority of the research focused on developing new synthetic polymers. One major limitation with these gene delivery vehicles though is that their molecular interactions with cells are poorly understood adding a layer of complexity to the development of efficient delivery vehicles.[3] Some barriers to successful nucleic acid delivery include cellular uptake, endosomal escape, and delivery efficiency of genetic material to the nucleus; therefore, polymers must be produced to overcome these known barriers so gene therapies can move forward in development.[3, 14-15]

2.1 Gene Delivery Mechanism

Though the full delivery mechanism and corresponding cellular interactions are not completely understood, the known barriers can be applied to the accepted gene delivery mechanism as illustrated in Figure 2.1. In order to produce efficient polymeric gene delivery vehicles, it is imperative to develop an understanding of this delivery mechanism.

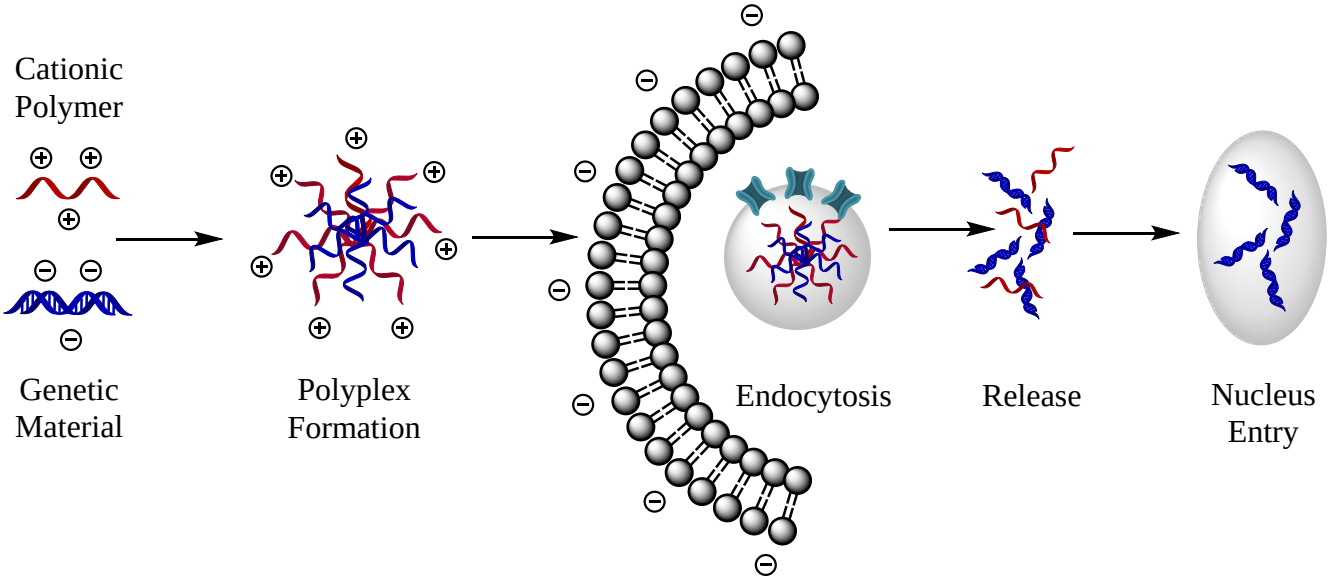

Figure 2.1 Mechanism for the delivery of genetic material by means of cationic polymer. Polymer and genetic material combine by electrostatic interactions, enter the cell by endocytosis, release into the cytoplasm, and the genetic material enters the nucleus.

The first step to gene delivery is the complexation of the delivery vehicle with the genetic material. Synthetic, cationic polymers are attracted to the negatively charged phosphate backbone of the genetic material by electrostatic interactions. The polymer and genetic material, once complexed, are termed a polyplex.[16] This polyplex, having an overall positive charge, is attracted to the negatively charged phospholipid bilayer of the cell exterior, again by electrostatic interactions. The polyplex then enters the cells by means of endocytosis. Once inside the cell, the genetic material and polymer are released into the cytoplasm leaving the genetic material to enter the nucleus and affect the cell[17]; the means of intracellular release, however, is under debate.

2.1.1 Proton Sponge Effect

There are multiple theories used to explain the endosomal escape pathway once the polyplex is taken up by the cell. One theory, termed the proton sponge effect, is illustrated in Figure 2.2. After endocytosis, the polyplex resides in an endosome which is known to facilitate degradation of foreign material; therefore, in order for the gene delivery vehicle to transport the genetic material to the nucleus, it must induce an endosomal escape mechanism.[17] To degrade foreign material, the endosome utilizes an ATPase proton pump enzyme to decrease the internal pH to acidic values of pH 5-6 moving it into the late endosomal stage. It then further traffics the material to a lysosome which has an even lower pH value of approximately 4.5.[17] Once the trafficking mechanism reaches this point, the polymer and genetic material cannot escape to the cytoplasm and are degraded. To overcome this endosomal trafficking and degradation, the gene delivery vehicle can be designed with cationic polymers of a desired pK_a value. Should the cationic polymer have a large number of titratable side chains, namely in the form of secondary or tertiary amines, the pK_a value can be tapered between the physiological pH and the pH of a lysosome. Once this cationic polymer enters the endosome, it will induce a larger influx of protons in order to protonate the amine groups. With this larger proton influx, comes a larger counter ion influx of chloride ions which then induces a larger intake of water molecules to compensate for the increased ion concentrations. It is this increase in water concentration that increases the osmotic pressure of the endosome eventually reaching a maximum point causing the endosome to burst. Once the endosome bursts, the genetic material is free in the cytoplasm to travel to the nucleus and obtain the desired biological activity.[17-19]

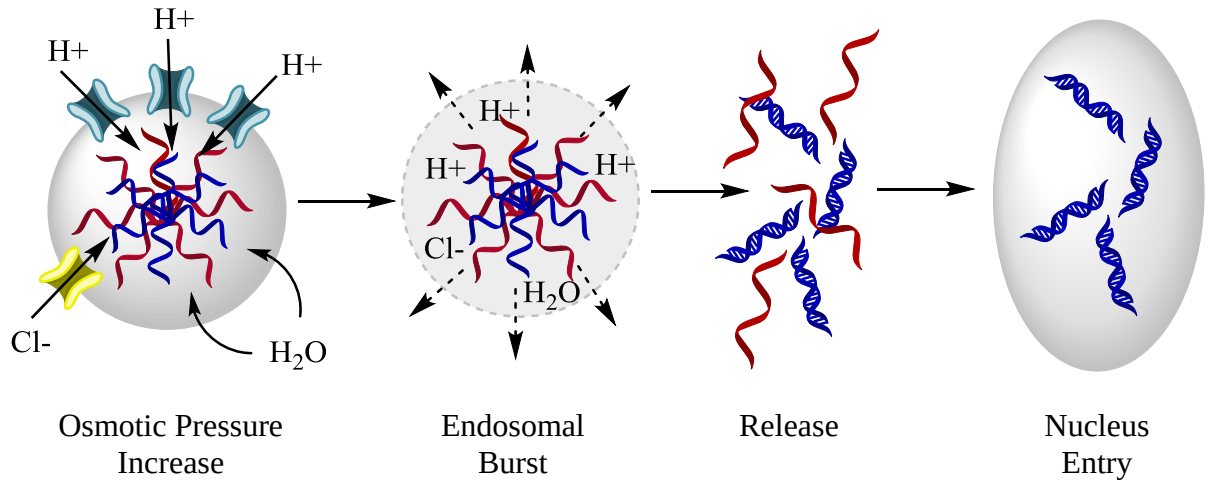

Figure 2.2 Mechanism for endosomal release as described by the proton sponge hypothesis.

2.2 Previous Studies

In order to take advantage of the endosomal escape mechanism by means of the proton sponge effect, certain cationic polymers have been extensively studied. Poly(ethyleneimine) (PEI), in particular, is known as the gold standard of cationic gene delivery vehicles since it has been reported to have high efficiency of polyplex formation as well as high gene expression[15, 20]; however, this purely cationic polymer induces immunogenic responses both *in vitro* and *in vivo* because of it nonspecific interactions with proteins and cells.[14-15, 21] Another limitation with utilizing cationic polymers such as PEI includes the lack of control over the molecular weight and architecture of the resulting polymers. Knowing these limitations, there is an inherent need to develop polymers with a hydrophilic section to impart polyplex stability and decrease cell toxicity as well as a need to develop or utilize a polymerization method that would afford control over the polymer synthesis in order to create polymers of well-defined molecular weights and architectures.

2.2.1 RAFT and Gene Delivery

With the advent of controlled radical polymerization (CRP), and more specifically RAFT polymerization, control over the synthesis of well-defined molecular weight polymers is now possible. Since the initial report on RAFT polymerization in 1998, many advances in the development of gene therapies have occurred. One significant adaptation of RAFT polymerization allowing for these advances is the ability to produce water-soluble, functional polymers, allowing not only the molecular weights and architectures of the polymers to be controlled, but biocompatibility of the polymer can also be afforded making RAFT polymerization ideal for developing gene delivery vehicles.[3-4, 10] A brief summary of the more common hydrophilic and pH-responsive monomers polymerized by RAFT and used for gene delivery purposes is shown in Figure 2.3 and Figure 2.4 respectively.[3, 10]

In the sections to follow, a number of previous works will be discussed. These publications report their findings on the RAFT synthesis of "smart" gene delivery vehicles. These copolymers are considered smart in that they contain a cationic moiety with a pK_a range around that of physiological conditions; therefore, they will respond to the pH gradient present in the endosomal pathway and induce the proton sponge effect. The first studies to be discussed will elucidate the effects of the addition and structural manipulation of the hydrophilic content to the gene delivery vehicle[22-24] while the remainder of this chapter will focus on varying the endosomolytic block to deduce their effects on the nucleic acid delivery efficiency.[28-31]

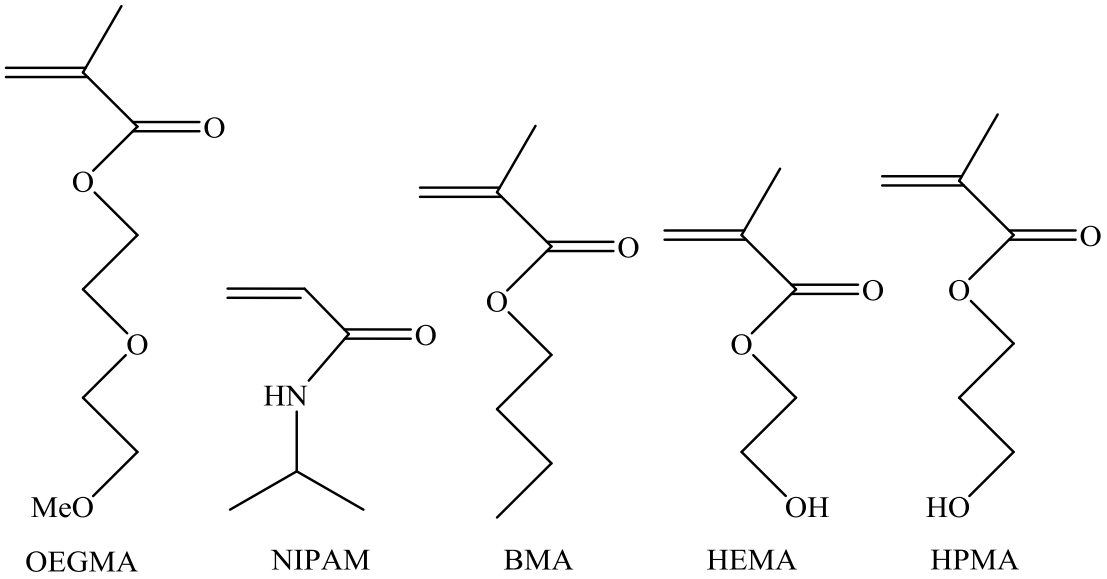

OEGMA NIPAM BMA HEMA HPMA

Figure 2.3 Hydrophilic monomers polymerized by RAFT for use in gene delivery vehicles. Oligo(ethylene glycol) methyl ether methacrylate (OEMGA), N-Isopropylacrylamide (NIPAM), Butyl methacrylate (BMA), 2-Hydroxyethyl methacrylate (HEMA), and 3-Hydroxypropyl methacrylamide (HPMA)

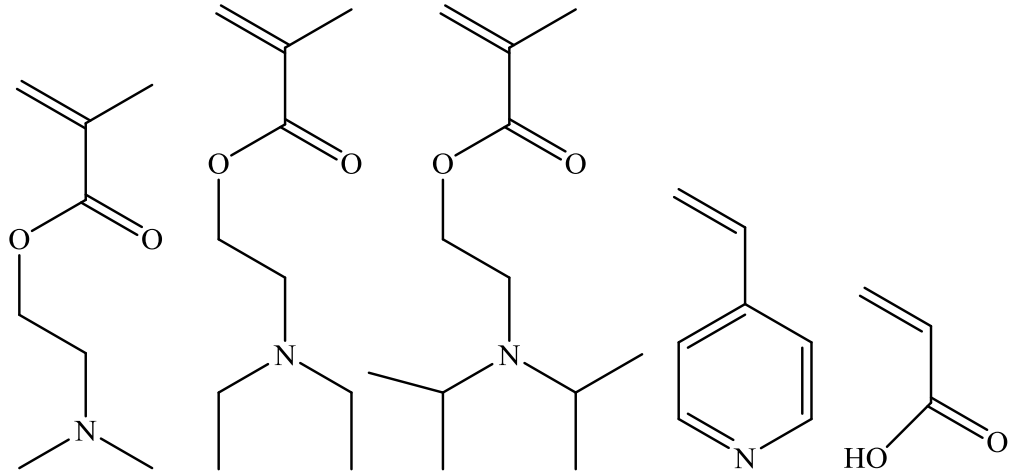

DMAEMA DEAEMA DPAEMA 4VP AA

Figure 2.4 pH-responsive monomers polymerized by RAFT for use in gene delivery vehicles. 2-Dimethylaminoethyl methacrylate (DMAEMA), 2-Diethylaminoethyl methacrylate (DEAEMA), 2-Diisopropylaminoethyl methacrylate (DPAEMA), 4-Vinyl pyridine (4VP), and Acrylic acid (AA)

2.2.2 Hydrophilic Architecture

PEI, though the gold standard for gene delivery, is known to induce an immunogenic response as a result of its nonspecific interactions with cells and proteins. In order to overcome this toxicity, it has been proposed to conjugate the cationic polymer with a hydrophilic, biocompatible polymer.[3, 14-15, 22-24] This hydrophilic segment then increases polyplex stability in physiological conditions as well as decreases cell toxicity making cationic polymers a more tenable for gene therapy use. One common way of improving the biocompatibility of the polymer is to incorporate poly(ethylene glycol) (PEG) into the copolymer design, eventually coining the term PEGylated copolymer.[22-24]

In 2002 and 2004, Deshpande et al. reported findings on PEGylated cationic copolymers containing the tertiary amine functionalized monomer 2-(dimethylamino) ethyl methacrylate (DMAEMA).[22-23] For this study the topology of the hydrophilic block was modified to elucidate its effect on gene delivery. Three different hydrophilic architectures were developed for this study by chain extending DMAEMA with different PEG-containing molecules as outlined in Table 2.1. Being linear in its natural state, PEG was utilized to develop a linear diblock copolymer as illustrated in Figure 2.5a. Two different PEG-functionalized polymers were then used to produce brush and comb-type copolymer structures. Poly(oligo(ethylene glycol) methyl ether methacrylate) (OEGMA) containing 7-8 PEG repeat units as side chains composed the hydrophilic content of the brush diblock copolymer (Figure 2.5b) while poly(ethylene glycol) methyl ether methacrylate (PEGMA) having 45 ethylene glycol repeat units as side chains was employed for the comb-type statistical copolymer (Figure 2.5c). Though PEG is present for all copolymers in this study, the percentage of this hydrophilic polymer differs among the different architectures. Since PEGMA contain PEG side chains 45 ethylene glycol units long, the degree of polymerization

of PEGMA as reported gives the statistical copolymer a higher overall PEG content as compared to the two diblock copolymers which contain similar hydrophilic content. Interestingly, the statistical copolymer also contains a larger number of DMAEMA repeat units giving the copolymer more protonatable side chains as compared to the diblock copolymers. Once synthesized, the copolymers were then studied *in vitro* in order to characterize and determine their gene delivery efficiency and cell toxicity. Three different cell lines, namely COS-7, human A549, and HepG2 cells, were used for the *in vitro* studies. From these characterization experiments, it was revealed that modification of the PEG architecture does have an effect on the gene delivery efficacy. Deshpande et al. reported similar transfection efficiencies for both the brush and linear diblock copolymers across all cell lines with the exception of the brush copolymer in the A549 cell line in which low gene expression was observed. The comb-type statistical copolymer, however, indicated low transfection efficiencies for all three cell lines. From a cytotoxic standpoint, the linear copolymer induced the most toxic effects resulting in the lowest cell viability of the copolymers studied; this polymer was also reported to have a concentration dependent toxicity with higher polymer concentration indicating lower cell viability. In contrast, both the block and statistical copolymers indicated similar high cell viability despite the polymer concentrations.[22-23]

Table 2.1 Properties of tertiary amine methacrylate polymers by Deshpande et al.[22-23]; m denotes the cationic degree of polymerization and n denotes the PEG-containing moiety degree of polymerization

Polymer	M_n	m	n	M_w/M_n
DMAEMA	5130	32	-	1.18
DMAEMA-OEGMA	8600	37	6-7	1.12
DMAEMA-PEG	7800	37	45	1.25
DMAEMA-stat-PEGMA	21000	66	5	1.11

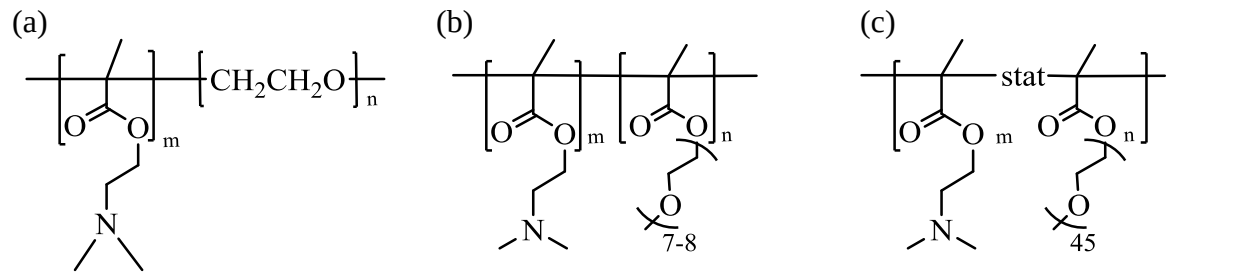

PEG_n-b-$p(DMAEMA)_m$ $p(OEGMA)_n$-b-$p(DMAEMA)_m$ $p(DMAEMA_m$-stat-$PEGMA_n)$

Figure 2.5 Structures of tertiary amine methacrylate polymers by Deshpande et al.[22-23]

In 2011, a similar study by Venkataraman et al. was published and reported findings on DMAEMA PEGylated copolymers.[24] For this study, the architecture of the hydrophilic block was again modified; however, the PEG weight fractions were similar among all polymers produced. The degree of polymerization of DMAEMA was also maintained to ensure the amount of cationic charge did not vary within the copolymer series. Like Deshpande, Venkataraman et al. aimed to define gene delivery efficiencies based solely on the topology of the PEG units. Here, PEG and OEGMA were again utilized for the linear diblock and brush diblock configurations respectively; however, unlike Deshpande, OEGMA was also utilized for the statistical copolymer. These hydrophilic polymers were then chain extended with DMAEMA to develop a series of PEGylated, cationic copolymers. In all, three copolymer structures were synthesized (Table 2.2). The generalized structure of these three polymers is outlined in Figure 2.6 while the synthesis illustrated in Scheme 2.1. After synthesis, the copolymers were then characterized *in vitro* to better understand their gene delivery efficiency and cell toxicity. Transfection experiments were carried out in both HEK293 and HepG2 cell lines to determine if the copolymer mediated transfection is cell type dependent. From these experiments, Venkataraman et al. also concluded that the PEG architecture has an effect on the gene delivery efficacy. Here, however, the reported trend indicated that the linear diblock copolymer induced higher gene expression as compared to the statistical

and brush block copolymers in both cell lines utilized. Interestingly, a cell dependent transfection efficiency was observed for all polymers with lower expression levels in the HepG2 cells. Cell toxicity was also studied utilizing the same two cell lines as in the transfection experiments, and cell dependent toxicity levels were reported. HEK293 cells were noted to have higher cell viability as compared to the HepG2 cells. Similar viabilities were observed for all copolymer architectures in the HEK293 cells; however, the polymers except the statistical comb-type copolymer induced a toxic effect in the HepG2 cells.[24]

Table 2.2 Characterization of compositionally equivalent and topologically different PEGylated cationic polymers by Venkataraman et al.[24]

Copolymer	$\bar{M}_n$ (Da)	PEG weight fraction	No. nitrogen atoms
mPEG-b-p(DMAEMA)	10100	0.20	49
p(DMAEMA-co-OEGMA)			
(a)	10700	0.24	46
(b)	15000	0.22	67
(c)	196000	0.23	90
p(OEGMA)-b-p(DMAEMA)	11800	0.22	53

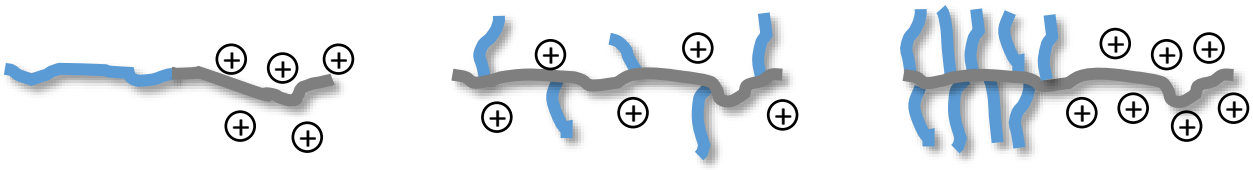

Figure 2.6 Schematic representation of model PEGylated cationic polymers containing different architectures of equivalent PEG components (represented by blue line) and comparable cationic components (represented by gray lines with positive charges) by Venkataraman et al.[24]

Scheme 2.1 RAFT polymerization-based synthetic route for the compositionally equivalent and topologically different PEGylated poly(dimethylaminoethyl methacrylate) based macromolecules, where the architecture of PEG chains was systematically varied to result in diblock copolymer (2), statistical copolymer (3a-c) and brush-block copolymer (5) by Venkataraman et al.[24]

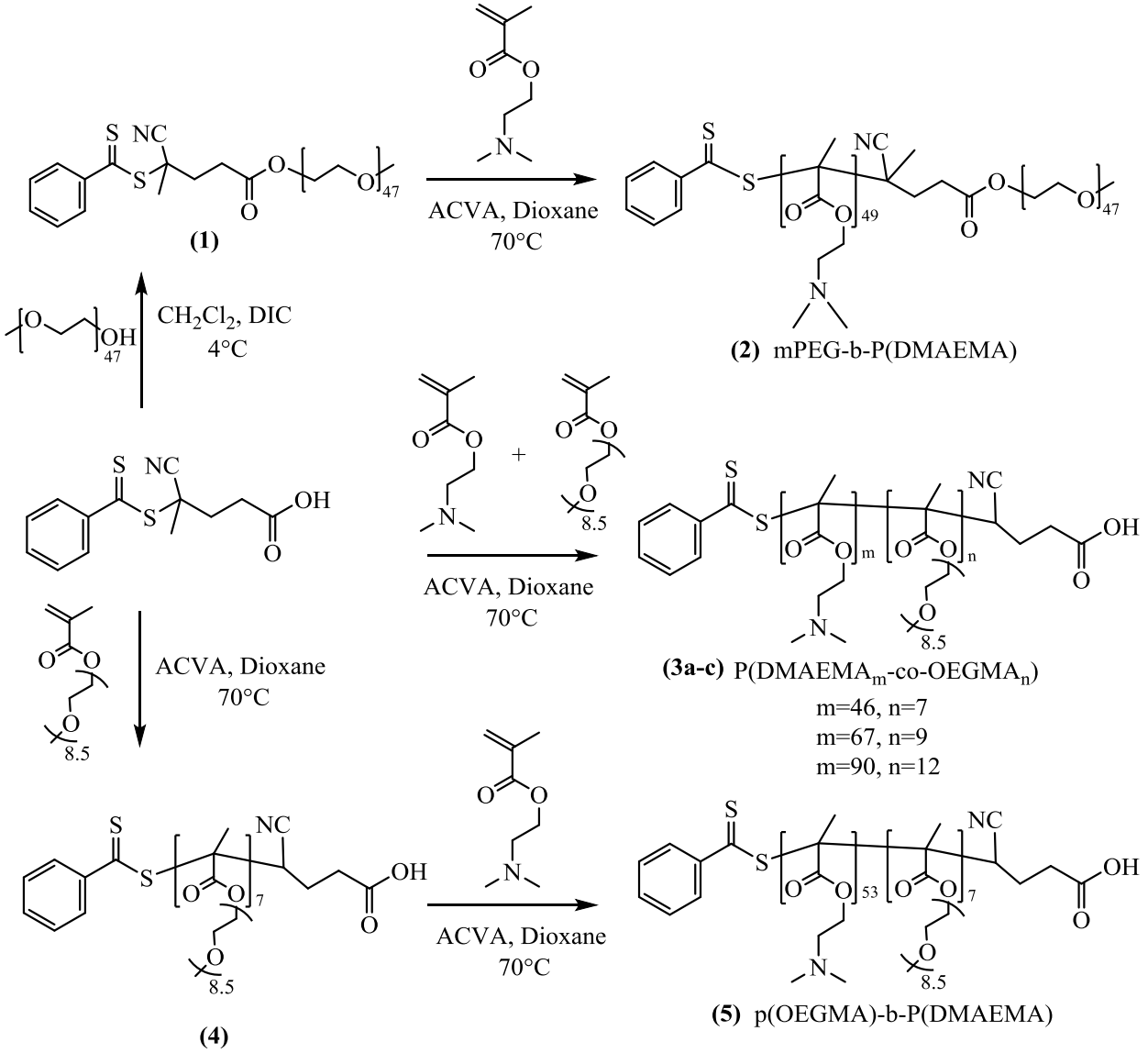

As a result of these studies, it was proposed that the architecture of the hydrophilic PEGylated content does have a significant effect on the transfection efficiencies of gene delivery vehicles. Though these works do disagree on overall trends indicated from transfection experiments, both authors conclude that the block topology, whether linear or brush-type, indicates

better nucleic acid delivery and gene expression than that of the statistical copolymer. As for cell viability, it was concluded that the copolymers have cell dependent toxic effects with the statistical copolymer inducing less of an immunogenic response as compared to the block topologies.[22-24] Additionally, it is worth noting that of the PEGylated molecules studied, only OEGMA and PEGMA can be synthesized with the polymerization control afforded by RAFT since they contain the needed reactive double bond. Therefore, moving forward, it would be advantageous to focus on utilizing OEGMA block copolymers for gene delivery purposes since these copolymers indicate low toxicity and high gene expression levels, and RAFT can be employed for synthesis purposes.

2.3.3 pH-Responsive, Cationic Polymers

Since it has been determined that PEGylation of cationic polymers increases the biocompatibility of the gene delivery vehicle, it now becomes imperative to develop polymers capable of successfully escaping the endosome before degradation. To produce such polymers, it is advantageous to utilize pH-responsive monomers capable of capitalizing on the proton sponge effect. Monomers that are considered pH-responsive are those that take advantage of a changing pH environment by altering their degree of ionization depending on the pH of the surrounding solution. For example, weak polyacids become more protonated by accepting protons at higher pH values while weak polybases become protonated at lower pH values. The actual ionic charge of the polyacids is negative at higher pH values while the opposite holds true for polybases in that they are positive at lower pH values.[10] Since the genetic material has a negative charge, it would be advantageous to further develop gene delivery vehicles utilizing polybases as they hold a positive charge in the lower pH values present in endosomes.

One type of pH-responsive monomer includes polybases containing a tertiary amine group. Of these tertiary amine containing monomers, DMAEMA has been the most extensively studied since the first reports of CRP and RAFT polymerization mainly due to its high transfection efficiencies and endosomal destabilizing properties.[25-27] The following studies to be discussed will focus on the RAFT polymerizations utilizing tertiary amine-containing monomers such as DMAEMA to synthesize gene delivery vehicles. The overall goal of this section is to deduce effects on how changing components of the endosomolytic block influences transfection efficiencies and cell toxicity.

In 2012, Hinton et al. published their work on the RAFT polymerization of ABA triblock copolymers designed for gene delivery. The copolymers were composed of the hydrophilic, PEG-functionalized monomer OEGMA (A-block) and the cationic DMAEMA monomer (B-block). Briefly, the DMAEMA macro chain transfer agent (macroCTA) was synthesized utilizing a bis-RAFT agent capable of producing the triblock copolymer functionality. The DMAEMA macroCTA was then chain extended with OEGMA in one of two different methods. The first of which utilized the raw product of macroCTA synthesis; therefore, DMAEMA monomers were still in solution and capable of copolymerizing with the OEGMA producing statistical A-blocks. For the second method the macroCTA was purified before chain extension with OEGMA; therefore, the resulting A-blocks consisted of pure hydrophilic content. Once synthesized, the copolymers then were subject to a quarternization reaction so that the DMAEMA repeat units would carry a permanent positive charge despite changing pH. Table 2.3 outlines a summary of the polymers synthesized for this study while Scheme 2.2 illustrates the polymerization schematic. The naming scheme found in Table 2.3 indicates the triblock architecture ABA followed by the number of PEG monomers/number of DMAEMA repeat units; Q indicates a quasi tri-block as synthesized from

polymerization method 1 while P indicates a pure tri-block synthesized from polymerization method 2. The triblock copolymers were synthesized with various A and B block lengths with the ultimate goal to determine the most efficient and least toxic copolymer structure. To characterize the ABA triblock copolymers, Hinton et al. utilized CHO-GFP and HEK293 cells to elucidate the copolymer effect on cell toxicity while only CHO-GFP cells were employed for cellular uptake and gene silencing assays. Hinton et al. reported that of the cationic B-block lengths studied, the range of DMAEMA repeat units between 110 and 120 was ideal for cellular uptake across the range of cells studied. Additionally, it was noted that decreasing the cationic block length caused a decrease in cellular uptake while increasing it caused an increase in cytotoxicity.

Table 2.3 The number average molecular weight, dispersity, and composition of the block copolymers prepared from DMAEMA and $OEGMA_{475}$ using RAFT polymerization from Hinton et al.[28]

ID*	Polymerization Method	Block B (PDMAEMA): molar mass (M_n in kDa)/ dispersity[a]	Tri-block ABA: molar mass (M_n in kDa)/ dispersity[a]	Number of repeat units in each block: A-B-A[b]	% of DMAEMA in A blocks
ABA-7/38Q	1	6.8/1.12	13.8/1.13	7-38-7	2.7
ABA-15/82Q	1	13.7/1.09	28.3/1.22	15-82-15	6.0
ABA-58/108P	2	17.9/1.15	73.1/1.72	58-108-58	0.0
ABA-69/113Q	1	18.6/1.17	84.6/1.75	69-113-69	5.5
ABA-33/110P	2	15.1/1.25	47.9/1.33	33-110-33	0.0
ABA-21/117Q	1	19.2/1.11	39.5/1.44	21-117-21	5.0
ABA-18/145Q	1	23.6/1.15	40.5/1.26	18-145-18	5.0
ABA-37/192Q	1	31.0/1.22	66.6/1.85	37-192-37	5.2

[a] As determined by gel permeation chromatography (GPC) against polystyrene standards.
[b] Calculated from GPC data before quarternization of the polymers.

Scheme 2.2 Reaction scheme representing the synthesis of RAFT-derived ABA tri-block copolymers by Hinton et al.[28]

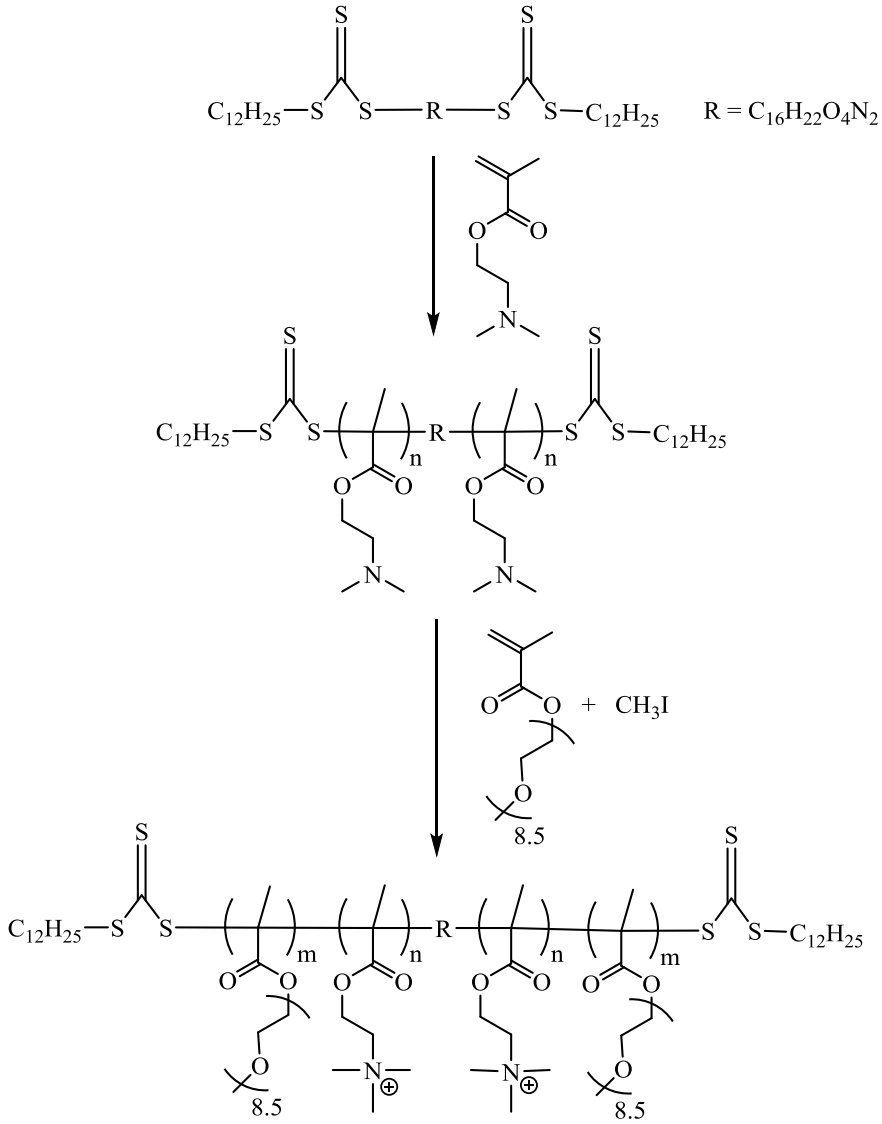

As for the varying OEGMA block lengths, it was concluded that all of the A-blocks with at least 15 OEGMA repeat units and some DMAEMA composition were efficient at delivering the genetic material. The authors postulate that this increased positive charge from incorporating DMAEMA into the hydrophilic blocks aids in the condensing of the genetic material. The positively charged DMAEMA units of the A-block are attracted to the negatively charged nucleic acids in the core of the polyplex making the entire complex aggregate more than if there were no

DMAEMA repeat units in the A-block; this attraction ultimately leads to better protection of the genetic material. In addition, the statistical copolymer being produced by the one pot method affords simplicity for the tri-block polymerization process since the intermediate purification step is not performed. Therefore, overall it was determined that an ABA triblock copolymer containing statistical A-blocks of hydrophilic and cationic content and a B-block of permanent positive charge yields the most efficient gene delivery vehicle.[28]

A study completed in a 2012 by Manganiello et al. analyzed the gene delivery efficiency of diblock copolymers composed of DMAEMA, 2-(diethylamino)ethyl methacrylate (DEAEMA), and butyl methacrylate (BMA). The DMAEMA macroCTA was synthesized and subsequently chain extended with various ratios of DEAEMA and BMA as shown in the reaction schematic in Scheme 2.3.

Scheme 2.3 RAFT-mediated synthesis of a diblock copolymer consisting of a cationic poly(DMAEMA) block and an endosomolytic hydrophobic block incorporating DEAEMA and BMA at varying molar feed ratios from Manganiello et al.[29]

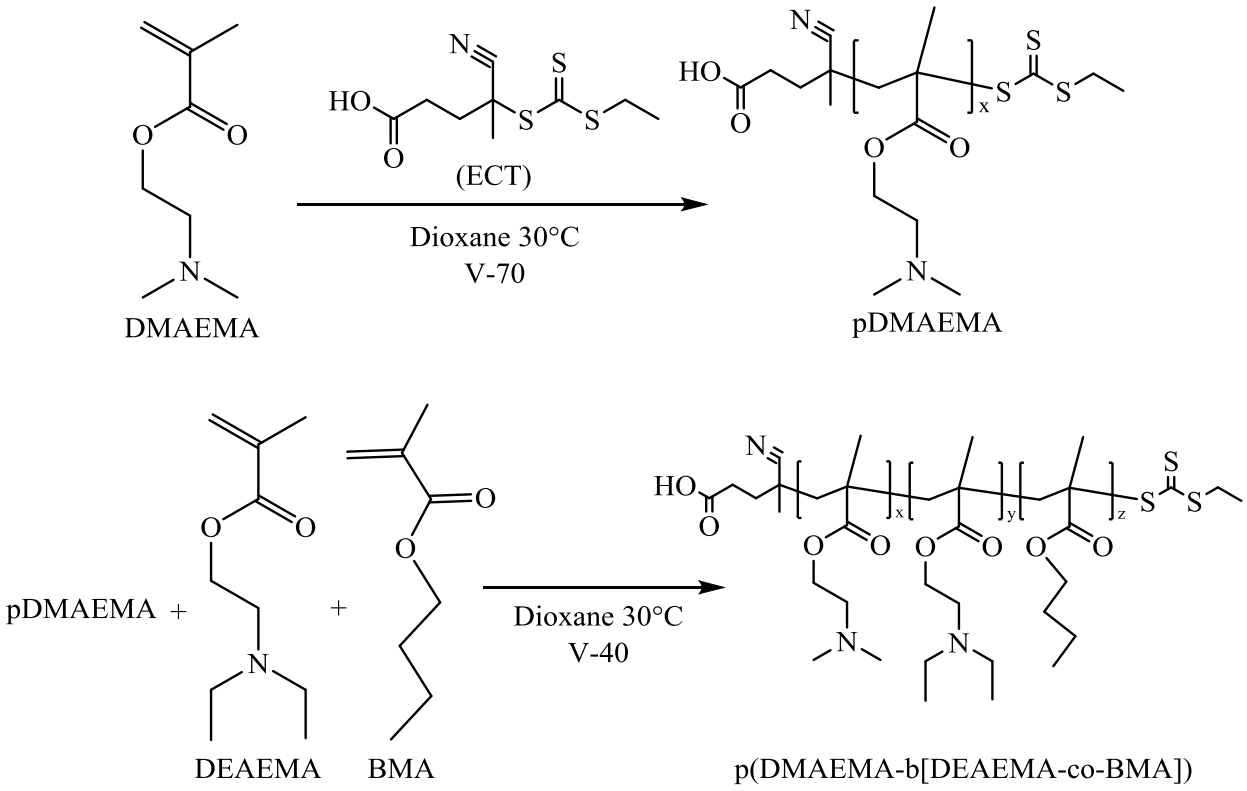

Unlike the previous studies utilizing DMAEMA for nucleic acid complexation, Manganiello utilized the DMAEMA block for polyplex formation as well as for hydrophilic stabilization as opposed to using a PEGylated monomer. The pH-responsive DEAEMA/BMA block was included for its endosomolytic activity. Like DMAMEA, DEAEMA also contains tertiary amine side chains capable of protonation in low pH environments; therefore, it can escape the endosomal pathway by the same mechanism. To deduce effects of added hydrophobic content to the endosomolytic block, the BMA percentages ranged from 20-70% in the B-block. These polymers having both cationic and hydrophobic content has a proposed endosomal escape mechanism in which the tertiary amine groups of DMAEMA and DEAEMA become protonated under decreasing pH conditions causing an increase in the positive charges of the polyplex core and corona. With DMAEMA being cationic as well, electrostatic repulsion will cause the polyplex to destabilize, therefore, releasing the genetic material. Additionally, increasing the hydrophobic content of the B-block causes the polyplex to be more stable since the hydrophobic moieties stay aggregated under aqueous conditions; therefore, by changing the DEAEMA to BMA ratio, the release mechanism could be optimized. After characterization experiments *in vitro* utilizing RAW264.7 and JAWSII cell lines, increasing transfection efficiency with decreasing BMA content was reported; however, this trend also holds true for cell toxicity with increasing toxicity for decreasing BMA content. Manganiello reported that copolymers containing 30-40% BMA content (60-70% DEAEMA) in the B-block exhibited the transition from inert to endosomolytic at those pH values expected in the endosome, providing the most promising gene delivery platform of the study.[29]

Scheme 2.4 RAFT-mediated synthesis of diblock copolymers consisting of a cationic poly(dimethylaminoethyl methacrylate) (DMAEMA, x=58) block and an endosomolytic polyampholyte block incorporating DMAEMA and propylacrylic acid (PAA) in equimolar ratios, and butyl methacrylate (BMA) (y~70) from Convertine et al.[30]

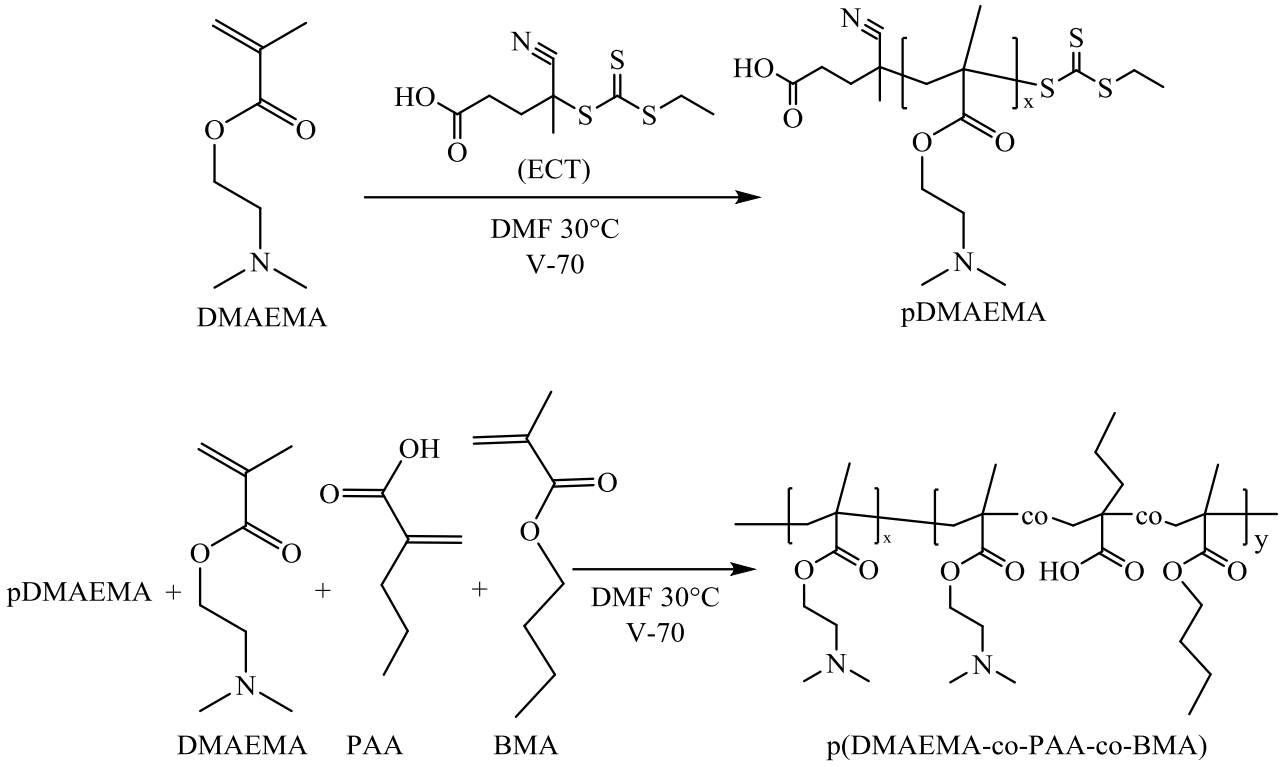

Similarly, in 2009 Convertine et al. reported on a copolymer family based on a comparable endosomal escape pathway to that of Manganiello.[30] In this study, a DMAEMA macroCTA was chain extended with varying ratios of DMAEMA, BMA, and propylacrylic acid (PAA) (Scheme 2.4). For the B-block, the feed ratios of DMAEMA and PAA were kept the same while the BMA content was varied. Again, DMAEMA is positively charged while BMA is hydrophobic. PAA, however, is negatively charged becoming protonated (less negatively charged) upon decreasing pH. Therefore, in the lower pH environments of the endosome, the PAA loses negative charge while the DMAEMA increases in positive charge, and by electrostatic repulsion among DMAEMA molecules, the polyplex is destabilized. The results of *in vitro* studies utilizing HeLa cells indicated that the polymer with the highest BMA content (50%) showed the highest level of

siRNA uptake. The cytotoxicity study indicated similar cell viability for all polymers analyzed in this study. As with Manganiello, Convertine et al. suspect a relationship between then BMA content of the endosomolytic block and the transfection efficiency of the copolymer.[30] Here, 50% BMA content was concluded as most the efficient polymeric gene delivery vehicle while Manganiello reported 30-40%.[29-30] The difference, however, can be explained by the different B-block content and endosomal escape mechanism of the these two studies.

In 2013 Nelson et al. reported on the PEGylated copolymers of DMAEMA copolymerized with BMA.[31] A linear PEG macroCTA was chain extended with various ratios of DMAEMA and BMA as illustrated in Scheme 2.5. The goal of this study was to identify a PEGylated gene delivery vehicle with an optimized B-block ratio of cationic and hydrophobic content. The previous studies, though analyzing the cation and hydrophobic ratios as well, did not include a PEGylated moiety for steric stability. From the studies in LR-3T3 and MDA-MB-231 cells, they noticed an inverse relationship between the BMA content in the polymer and the transitional pH of the micelles. The greater the BMA content, the lower the pH of the surrounding environment needed to be in order to induce the endosomolytic activity. This same trend was recognized and reported in both reports by Manganiello et al. and Convertine et al.[29-30] The conclusion of the study by Nelson et al. was the copolymer containing 50% BMA has the optimum ratio of positive charge to hydrophobicity and efficiently delivers the genetic material to induce a biological response.[31]

Scheme 2.5 Polymer synthesis scheme for PEG-(DMAEMA-co-BMA) from Nelson et al.[31]

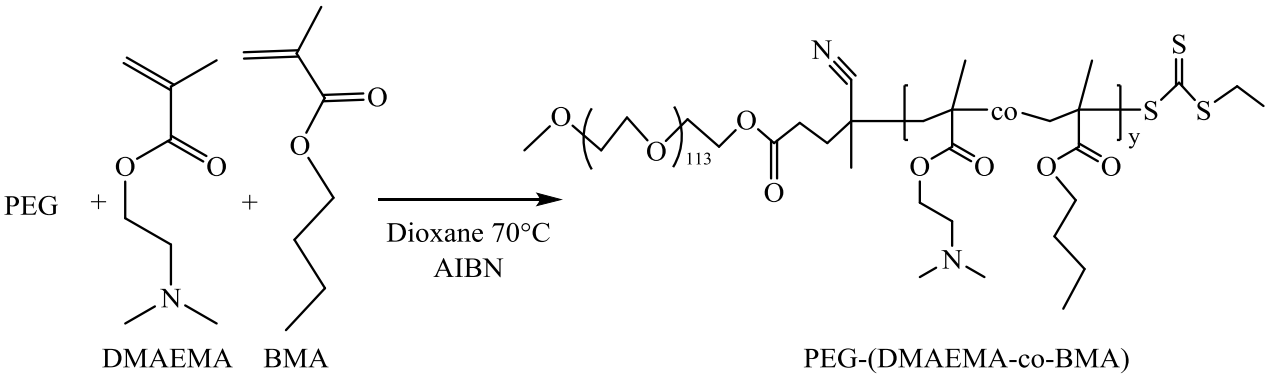

Much research has been reported on the gene delivery efficacies of polymeric gene delivery vehicles. With the advent of CRP methods and RAFT polymerization in particular, it is now possible to synthesize polymers of well-defined molecular weights and architectures as well as biocompatible polymers containing hydrophilic segments for polyplex stability and toxicity control. Upon analysis of the previous works presented in this chapter, it is apparent that PEGylation of cationic polymers affords a biologically compatible copolymer ideal for gene delivery purposes. The addition of hydrophobic content in the cationic block of a copolymer has also been reported to increase the gene delivery efficacy. Interestingly, the variance of the cationic block without hydrophobic content is yet to be extensively studied or reported; therefore, it would be a worthwhile study to deduce the effects of cationic content and functionality on the gene delivery efficiency and cell toxicity.

CHAPTER 3

RAFT POLYMERIZATION FOR THE SYNTHESIS OF TERTIARY AMINE-BASED DIBLOCK COPOLYMER NUCLEIC ACID DELIVERY VEHICLES

3.1 Abstract

A wide range of nucleic acid delivery vehicles have been studied for their efficacy in gene therapy, and with advances in controlled radical polymerization (CRP) techniques, the synthesis of precise polymeric architectures needed for these delivery vehicles is now possible. The development of a family of pH-responsive, diblock copolymers designed to effectively delivery genetic material is reported. The polymers were prepared by RAFT polymerization utilizing an oligo(ethylene glycol) methyl ether methacrylate (OEGMA) stabilizing block and a cationic block derived from a family of pH-responsive, tertiary amine-containing methacrylates, namely 2-(dimethylamino) ethyl methacrylate (DMAEMA), 2-(diethylamino) ethyl methacrylate (DEAEMA), 2-(diisopropylamino) ethyl methacrylate (DPAEMA), capable of complexing with negatively charged nucleic acids. Nine copolymers were synthesized utilizing the same hydrophilic block length while varying the degree of polymerization of the cationic block to lengths of 25, 50, and 75 monomer units. The polymers were characterized by gel permeation chromatography (GPC) to determine their molecular weight and polydispersity. To characterize the binding affinity of the siRNA/polymer complexes, electrophoresis and dynamic light scattering (DLS) experiments were carried out in various pH environments to mimic the pH values present in the early and late endosome. The diblock copolymers condensed siRNA at all N/P ratios at pH

5, while less binding affinity was observed with increasing pH. At all pH values, the polyplexes indicated particle sizes less than 25 nm in diameter, ideal for cell entry. *In vitro* studies utilizing HEK293 and MCF-7 cells were employed to evaluate cell toxicity and determine polymeric gene delivery efficiency. The cytotoxicity study indicates high cell viability with the diblock copolymers with the exception of E50 and E75 while the gene knockdown experiments indicated high siRNA delivery efficiency for all nine copolymers. As a result, this copolymer family will enable further studies and development for promising gene delivery vehicles capable for clinical use.

3.2 Introduction

Since the emergence of gene therapy, a number of gene delivery vehicles have been characterized for their gene delivery efficacies.[3, 10, 32-33] It has been reported from various studies that viral vectors indicate high toxicity and immunogenicity; therefore, the development of non-viral vectors is crucial to the progression and clinical use of gene therapy.[14-15, 33] Non-viral gene delivery vehicles such as cationic lipids and polymers have been extensively studied with reports of high transfection efficiencies; however, a number of these studies have failed during clinical trials.[14-15] The challenges associated with utilizing non-viral vectors as gene delivery vehicles are mainly due to the lack of knowledge or understanding of their molecular interactions with cells and the overall gene delivery mechanism. Some known barriers to further developing polymeric gene delivery vehicles include cellular uptake, endosomal escape, and the efficient delivery of genetic material to the nucleus.[14-15, 34] To overcome these challenges, pH-responsive polymers such as poly(ethyleneimine) (PEI) have been developed and studied for their ability to capitalize on the pH gradients of the endosomal pathway.[35] Though PEI is known to have high efficiency of

polyplex formation as well as high gene expression, this polymer induces immunogenic responses both *in vitro* and *in vivo* because of it nonspecific interactions with various proteins and cells.[14-15] Moreover, there is a lack of control over the resulting molecular weight and architecture of PEI and other cationic polymers utilized for gene delivery vehicles.[4, 36] These limitations of biocompatibility and polymerization control have stimulated further research and development of alternative polymeric gene delivery vehicles.

In order to improve the biocompatibility of cationic polymers for gene delivery, a hydrophilic component such as poly(ethylene glycol) (PEG) can be incorporated into the polymer design to afford stability in aqueous environments.[3, 22-24, 31] A number of studies have discussed the positive effects of PEGylated copolymers on gene delivery efficiency with results including the decrease in immunogenicity and cellular toxicity and overall improvement in the polyplex stability *in vitro*.[22-24] Studies such as those by Deshpande et al. and Venkataraman et al. have reported that varying the PEG architecture has an effect on the delivery efficiency of genetic material and indicate that a block copolymer structure has better delivery efficiency than that of a statistical copolymer.[22-24]

With the advent of controlled radical polymerization (CRP) techniques, reversible addition-fragmentation chain transfer (RAFT) polymerization in particular, the synthesis of well-defined molecular weight polymers with low polydispersity is now possible.[1-2] One significant adaptation of RAFT polymerization is the advancement in the ability to produce water-soluble, functional polymers that are inherently biocompatible, ideal for the development of gene delivery vehicles.[3-4, 10] Many studies have reported on the use of tertiary amine-containing monomers for use as the cationic building blocks for gene delivery vehicles. Of these, DMAEMA has been the most extensively studied since the first reports of CRP and RAFT polymerization due to its high

transfection efficiency and endosomal destabilizing properties.[25-27, 37] A number of studies have elucidated the effects of PEGylated DMAEMA polymers with incorporated hydrophobic content as effective gene delivery vehicles.[28, 31] The role of tertiary amine functionality alone on the nucleic acid delivery efficiency has yet to be discussed.

Here, we report on the biological efficacy of a series of diblock copolymer gene delivery vehicles. Utilizing RAFT polymerization to ensure the controlled synthesis of well-defined block copolymers with narrow PDIs, we designed and synthesized a family of tertiary amine-based PEGylated copolymers incorporating oligo(ethylene glycol) methyl ether methacrylate (OEGMA) to promote biocompatibility as well as colloidal stability and 2-(dimethylamino) ethyl methacrylate (DMAEMA), 2-(diethylamino) ethyl methacrylate (DEAEMA), or 2-(diisopropylamino) ethyl methacrylate (DPAEMA) for nucleic acid complexation and endosomal escape. To examine the effects of cationic functional groups and block length on gene delivery efficiency, nine diblock copolymers were synthesized with varying degrees of polymerization in order to analyze and elucidate the effects of different cationic moieties on polyplex formation and *in vitro* delivery.

3.3 Experimental Procedures

3.3.1 Materials

All chemicals were purchased from Sigma-Aldrich at the highest available purity and used as received unless otherwise noted. OEGMA (M_n = 475 g/mol), DMAEMA, DEAEMA, DPAEMA were passed through a column of basic alumina to remove inhibitor prior to polymerization.

3.3.2 Polymer Synthesis

Utilizing RAFT polymerization, a solution of OEGMA (59.4 g, 125 mmol), 4-cyano-4-[(dodecylsulfanylthiocarbonyl)sulfanyl] pentanoic acid (CDP) (1.01 g, 2.5 mmol), and 4,4'-azobis(4-cyanovaleric acid) (V-501) (140 mg, 0.5 mmol) in 445 mL DMSO were added to a 1000 mL round bottom flask fitted with a rubber stopper. This solution was sparged with nitrogen for 30 minutes and placed in a 70°C preheated oil bath. The polymerization was allowed to proceed for 2 hours prior to termination by exposure to air. The resulting polymer was purified by dialysis against water for 3 days and then subsequently recovered by lyophilization.

The resulting OEGMA macroCTA was chain extended with DMAEMA (pK_a 7.4), DEAEMA (pK_a 7.2), or DPAEMA (pK_a 6.9) to form the desired block copolymers. For all block copolymerizations, the $[M]_o/[CTA]_o$ and $[CTA]_o/[I]_o$ were 125:1 and 10:1 respectively. As an example, a solution of DMAEMA (2.36 g, 15 mmol), pOEGMA macroCTA (2.2 g), and V-501 (3.4 mg, 0.012 mmol) in 12.5 mL of DMF was added to a 40 mL glass reaction vial fitted with a septa cap. The solutions were sparged with nitrogen for 20 minutes prior to polymerization in a 70°C preheated Thermo Scientific MaxQ 2000 Shaker coupled with a J-KEM temperature controller. The polymerization was allowed to proceed for 2.75 hours prior to termination by exposure to air. The resulting diblock copolymer, p(OEGMA-*b*-DMAEMA), was purified by dialysis against DI water for three days prior to lyophilization.

3.3.3 Polymer Characterization

Gel permeation chromatography (GPC) was used to determine the number-average molecular weight (M_n) and polydispersity indices (PDIs) of the diblock copolymers. Utilizing a Thermo Scientific Dionex pump (UltiMate 3000 Pump) and paired autosampler (UltiMate 3000

Autosampler Column Compartment), an aqueous eluent of 1 wt% acetic acid/ 0.10 M Na_2SO_4 (aq) at a flow rate of 0.25 mL/min was employed. Eprogen Inc. columns [CATSEC 1000 (7 μ, 50 x 4.6), CATSEC 100 (5 μ, 250 x 4.6), and two CATSEC 300 (5 μ, 250 x 4.6)] connected in series were coupled with a Wyatt miniDAWN TREOS multi-angle light scattering detector (λ = 690 nm) and a Wyatt Optilab t-REX differential refractive index (dRI) detector (λ = 690 nm). The dn/dc of each homopolymer was measured utilizing the Wyatt Optilab t-REX; dn/dc values were implemented into the Wyatt Technology ASTRA software calculations for absolute molecular weight determination.

3.3.4 siRNA/Copolymer Complex Characterization

To verify the stable siRNA/polymer complexation, agarose gel electrophoresis was utilized. A 46 nucleotide, single-stranded oligonucleotide comprised of the NHE III_1 region of the MYC promoter and labeled with the fluorescent dye Fluorescein (6-FAM) (0.25 μM, sequence: 5'-GCGCTTATGGGGAGGGTGGGGAGGGTGGGGAAGGTGGGGAGGAGAC-3') was mixed with aqueous solutions of the diblock copolymers in Tris-Acetate EDTA (TAE) buffer at pH values of 5,7, or 9. The theoretical charge ratio of the nitrogen in the polymers to phosphorous in the nucleic acids (N/P) were calculated using the positively charged cationic blocks of DMAEMA, DEAEMA, or DPAEMA and the negatively charged siRNA. N/P ratios ranging from 0 to 7 were utilized. The copolymer/siRNA mixtures were allowed to incubate for 30 minutes at room temperature to allow for polyplex formation before 3μL of 50% glycerol and 1 μL of 6x DNA loading dye were added. The polyplex samples were then loaded on 1% agarose gels with 1x GelGreen dye (Phenix Research, Candler, NC) made with TAE buffers at the same pH as

incubation. Gels were subjected to 70V for 30 minutes before transillumination imaging on a FotoDyne gel imager.

The size of the siRNA/copolymer complexes were characterized in varying pH solutions by dynamic light scattering (DLS) utilizing a Malvern Zetasizer Nano ZS (Malvern Instruments Ltd., Max 4 mW He-Ne laser, incident beam λ=633 nm) and accompanying Zetasizer Software. Briefly, copolymers were incubated in water (pH 5, 7, and 9) with appropriate amounts of 6-FAM (0.3 μM) at an N/P ratio of 3. Copolymers were allowed to condense the siRNA for 30 minutes at room temperature before running measurements in triplet.

3.3.5 Cellular Uptake

To initially determine if this copolymer series was capable of cellular transfection, the polymer/siRNA complexes were incubated with human embryonic kidney cells (HEK293) maintained in a 37°C humid atmosphere containing 5% CO_2. To measure the cellular uptake, cells were seeded in 12-well plates at a concentration of 1 x 10^5 cells per well in 1 mL of media. The cells were allowed to incubate overnight before addition of polymer/siRNA complexes. The next day, polyplexes at an N/P ratio of 3 were prepared utilizing a 19-mer fluorescein-labeled scramble siRNA (0.545 μM, Cell Signaling Technology) and the appropriate amounts of copolymer solution and the reduced serum media Opti-MEM (GIBCO). The mixture was subsequently allowed to incubate at room temperature for 30 minutes. Additionally, the siRNA was incubated at room temperature with 1.2 μL of Fugene (Promega). The polyplexes and Fugene/siRNA complexes were then added to the wells and allowed to incubate for 24 hours. The next day the media was discarded and replaced to rid any free polymer or siRNA. The efficiency of the copolymer mediated gene delivery was then qualitatively determined with use of a fluorescent enabled

microscope by visualizing the fluorescence of the Fluorescein labeled siRNA that was successfully delivered to the cells.

3.3.6 Cell Viability Assay

MCF-7 cells were seeded in 96-well plates at a concentration of 7.5×10^3 cells per well in 90 μL of media and were allowed to attach overnight. The following day, a 10x stock plate of polyplex solutions diluted from 5 mM over a 5-6 log range in 0.5 log steps was made, and 10 μL of this stock was added to the cell plate, in triplicate. The final high dose range was 0.08 – 500 μM. Cell-free wells with the same dose-range were plated, and served as measurements of background absorption. 48 hr later, 20 μL of MTS + 5% PMS was added to each well and incubated for ~2 hr before the absorption at 490 nm was measured on a BioTek Synergy 2 plate reader (Winooski, VT). Background absorptions were subtracted, and data were normalized to control cells to determine any changes in cell viability.

3.3.7 MYC Knockdown Studies

MCF-7 breast cancer cells were obtained fresh from ATCC (Manassa, VA) and were maintained in exponential growth in Dulbecco's minimal essential medium (DMEM) that was supplemented with 10% fetal bovine serum and 1x penicillin/streptomycin solution in a 37°C humid atmosphere containing 5% CO_2. To measure cellular uptake, cells were seeded in two 12-well plates at a concentration of 8×10^4 cells per well in 0.5 mL of media and allowed to attach overnight. The following day, polyplexes were prepared as previously described with a 19-mer MYC siRNA (Cell Signaling Technology, #6341) at an N/P ratio of 3. In addition, the siRNA was complexed with 1.2 μL of Fugene HD (Promega) and incubated for 30 minutes at room

temperature. The polyplexes were added to the wells and allowed to incubate for 48 hr. After the 48 hour period, the wells were rinsed with water, and the cells were collected by lysis buffer. After subsequent β-mercaptoethanol (BME) addition, all samples were frozen for future analysis.

Once samples were thawed, the RNA was extracted with the use of a Roche GeneJET kit (Roche, Basel, Switzerland) according to the kit directions. The yield and purity of the RNA was determined with the use of a NanoDrop-1000 (NanoDrop); only samples with 260/230 values greater than 1.5 were considered pure enough for continued use. 500 ng of RNA was reverse transcribed into cDNA using the BioRad iScript kit according to the directions using a BioRad Thermocycler. Quantitative polymerase chain reaction (qPCR) was run on the cDNA samples using TaqMan primers (ABI). In particular, 5 μL of cDNA was evaluated by multiplexing FAM-labeled MYC primers (Life Technologies, Hs00153408_m1) with VIC-labeled GAPDH primers (Life Technologies, catalog number 4326317E) using SsoAdvanced PCR Mix (BioRad) on a CFX Connect qPCR machine (BioRad). Changes in RNA expression were determined by the $\Delta\Delta C_q$ method.

3.4 Results and Discussion

3.4.1 Polymer Synthesis

RAFT polymerization enabled the synthesis of well-defined AB diblock copolymers for nucleic acid delivery. The pH-responsive diblock copolymers were synthesized according to Scheme 3.1. The RAFT polymerization of OEGMA was initiated by V-501 and mediated by CDP in DMSO. After purification, the OEGMA macroCTA was chain-extended with one of three tertiary amine monomers, DMAEMA, DEAEMA, or DPAEMA, to yield a series of diblock

copolymers with a permanently hydrophilic A block to impart water-solubility and provide steric hindrance to aggregation and varying lengths of pH-responsive B blocks for nucleic acid complexation. The degrees of polymerization of 25, 50, and 75 were targeted for the pH-responsive B block in order to investigate the effect of the repeat unit structure and block length of the cationic block on the delivery of nucleic acid payloads.

Scheme 3.1. RAFT polymerization of OEGMA and subsequent chain extension with tertiary amine-containing monomers to form pH-responsive diblock copolymers for siRNA delivery.

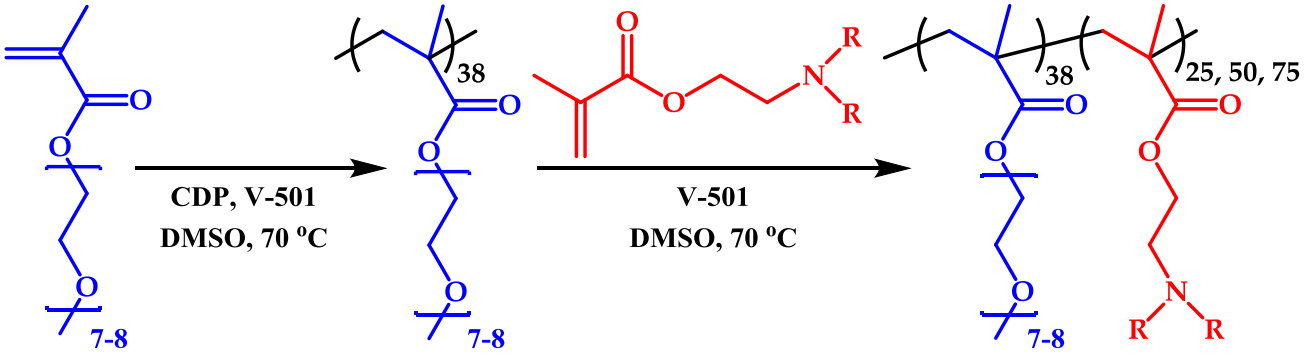

3.4.2 Polymer Characterization

RAFT polymerization proved to be an effective methodology for controlling the degrees of polymerization of the diblock copolymers while maintaining a low polydispersity index (< 1.1) as shown in Table 3.1. To prove the successful chain extension of the OEGMA macroCTA, GPC chromatograms of the macroCTA and P75 are depicted in Figure 3.1. P75 has a shorter elution time as compared to the OEGMA macroCTA; therefore, P75 has a larger molecular weight indicating the desired chain extension of the macroCTA and successful synthesis of amphiphilic diblock copolymers. The slight tail observed with the P75 chromatogram can be attributed to a small percentage of dead macroCTA polymer chains not capable of chain extension.

Table 3.1. Molecular weight data for the pH-responsive diblock copolymer series.

	Polymer	M_n (g/mol)	PDI
p(OEGMA$_{38}$-*b*-DMAEMA$_{27}$)	M25	22,900	1.02
p(OEGMA$_{38}$-*b*-DMAEMA$_{51}$)	M50	26,800	1.02
p(OEGMA$_{38}$-*b*-DMAEMA$_{76}$)	M75	30,800	1.01
p(OEGMA$_{38}$-*b*-DEAEMA$_{29}$)	E25	24,400	1.03
p(OEGMA$_{38}$-*b*-DEAEMA$_{50}$)	E50	28,800	1.05
p(OEGMA$_{38}$-*b*-DEAEMA$_{73}$)	E75	33,900	1.04
p(OEGMA$_{38}$-*b*-DPAEMA$_{29}$)	P25	26,600	1.04
p(OEGMA$_{38}$-*b*-DPAEMA$_{53}$)	P50	32,800	1.04
p(OEGMA$_{38}$-*b*-DPAEMA$_{74}$)	P75	38,300	1.02

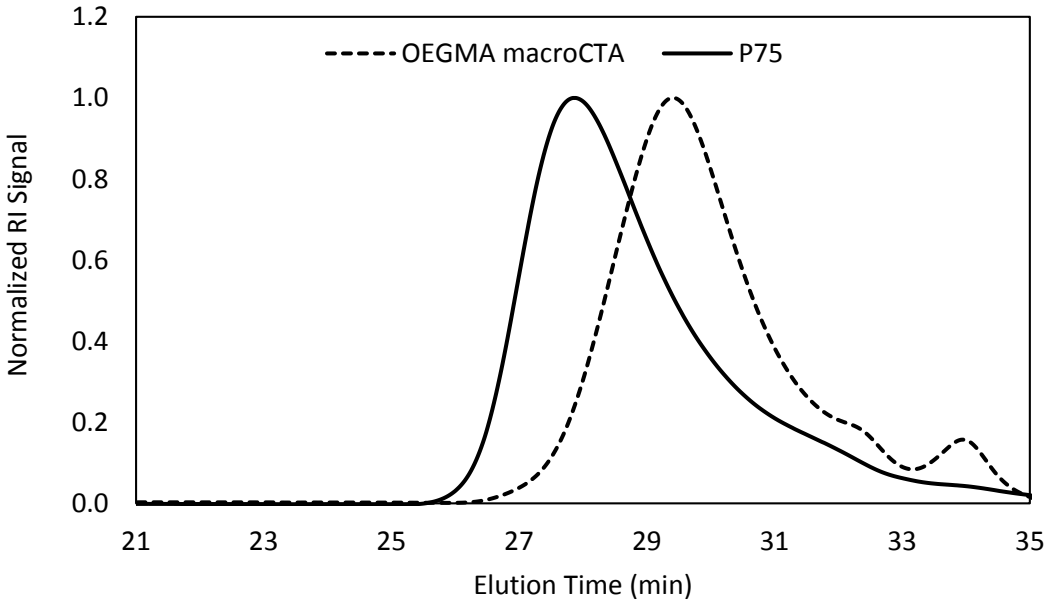

Figure 3.1. GPC chromatogram indicating the successful chain extension of the OEGMA macroCTA with DPAEMA. The P75 copolymer has a shorter elution time from the GPC columns indicating that it has a larger molecular weight than the macroCTA.

3.4.3 siRNA/Copolymer Characterization

The ability of the pH-responsive diblock copolymers to bind with nucleic acids was assessed via electrophoretic gel shift assays. The three protonatable tertiary amine-contianing B-

blocks have pKa values varying from 6.9 for DPAEMA to 7.4 for DMAEMA. We tested the nucleic acid binding abilty of the diblock copolymers at pH values of 5, 7, and 9 to examine the pH effect on the binding affinity of the diblock copolymers. Figure 3.2 shows a representative series of gel shift assays for the diblock copolymers with a targeted B block degree of polymerizaiton of 50.

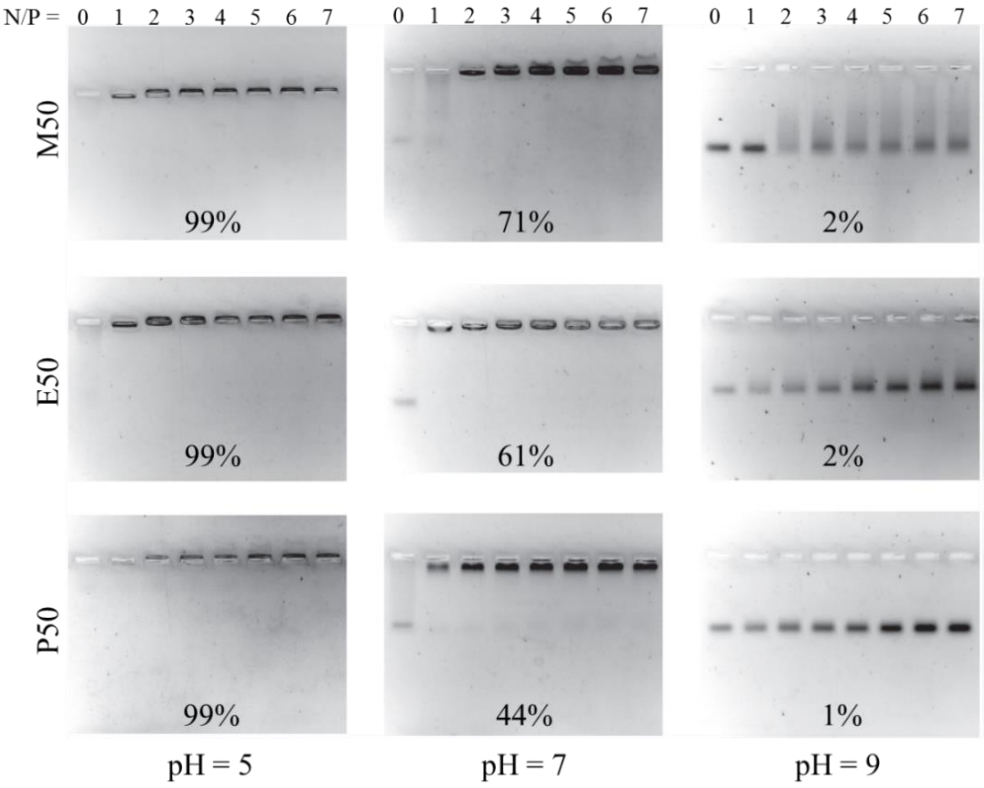

Figure 3.2 Gel shift assays for the diblock copolymers M50, E50, and P50. pH values of 5, 7, and 9 with N/P ratios ranging from 0 (no polymer added) to 7 were utilized. The percent of the B block moieties protonated is shown for each gel shift experiment.

At a pH of 5 where ~ 99% of the tertiary amine moieties are protonated, M50, E50, and P50 bind DNA at the low N/P ratio of 1 indicted by the fluorescent signal remaning in the wells. The somewhat low florescense signal for all samples at pH 5 can be explained by the reported effect of low pH environments on the fluoresnce of molecules including Fluroroscein[38]. If the pH

value of the buffer is increased to 7, the percentage of protonated tertiary amine moieties decreases, but has only a minimal effect, if any, on the nucleic acid binding. As the pH of the buffer is further increased to a value of 9, the tertiary amine groups become mostly deprotonated (>98%) and has a dramatic effect on the ability of the diblock copolymers to complex with nucleic acids. For all diblock copolymers tested at pH 9, minimal NA binding was observed for all tested N/P ratios 0 to 7.

To further characterize the siRNA/copolymer, DLS was employed to analyze the pH-dependent nature of the copolymers by determining the polyplex size at varying pH. Utilizing a theoretical charge ratio of 3:1, the polymers and nucleic acid material were allowed to incubate in water at pH 5, 7, and 9 before DLS measurements. From this characterization, it was determined that the polyplex diameter at pH 5, 7, and 9 for all copolymers investigated was less than 25 nm making them ideal for cellular uptake. As an example, Figure 3.3 illustrates the DLS data for M50 complexed with siRNA in water at pH 5, 7, and 9. A shift to larger diameters with increasing pH is expected and observed. When not complexed with genetic material, the pKa of DMAEMA is 7.4. At the lower pH, therefore, the vast majority of the tertiary amines would be protonated causing the siRNA/polymer complexes to be more tightly bound. This strong binding affinity is indicated by the smaller diameter in the pH 5 solution. The polyplex size then increases with increasing pH since less of the tertiary amine side chains will be protonated. This decrease in positively charged moieties causes the polyplex to have less molecular interactions with the nucleic acids which in turn causes the polyplex to swell indicated by the larger particle size.

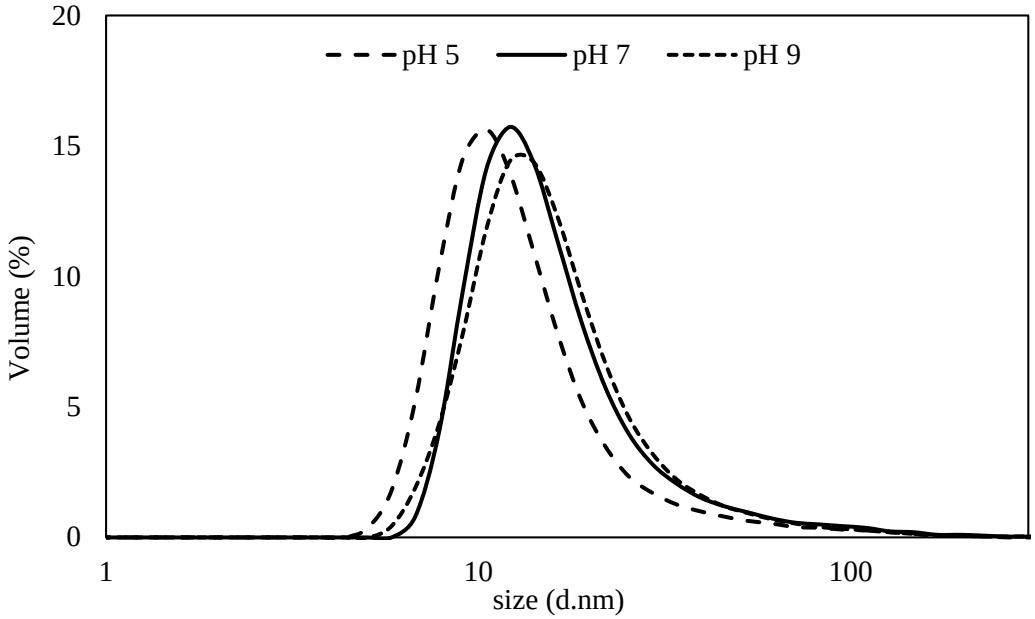

Figure 3.3 DLS measurements of M50 characterizing the pH-responsive nature of the tertiary amine-based polymers. The data shows that for increasing pH, the polyplex diameter increases as well indicating the pH dependent behavior of this diblock copolymer family.

3.4.4 siRNA/Copolymer Cellular Uptake

The ability of the copolymers to deliver genetic material to cells at an N/P ratio of 3 was determined by the *in vitro* experiments utilizing the HEK293 cell line. This *in vitro* study was utilized to gain preliminary results of the polymer-mediated gene delivery efficiency in order determine if the copolymer series should be further pursued with more mature studies and experimentation. The polymers were incubated with the siRNA for thirty minutes to allow for polyplex formation before being added to the cell culture to incubate for 24 hours. After this period, the fluorescent levels of fluorescein were qualitatively evaluated utilizing a fluorescent enabled microscope. The images collected from this copolymer mediated cellular uptake study are shown in Figure 3.4 along with the two controls of siRNA only and Fugene mediated delivery. Overall, we noticed some degree of fluorescence with all nine cultures indicative of successful polymeric nucleic acid delivery; however, E50, P50, and P75 visually appear to have delivered the highest

concentration of the nucleic acid material, as indicated by the stronger fluorescence signal. Though further investigations would be required, we know this copolymer series is capable of effectively delivering genetic material to HEK293 cells.

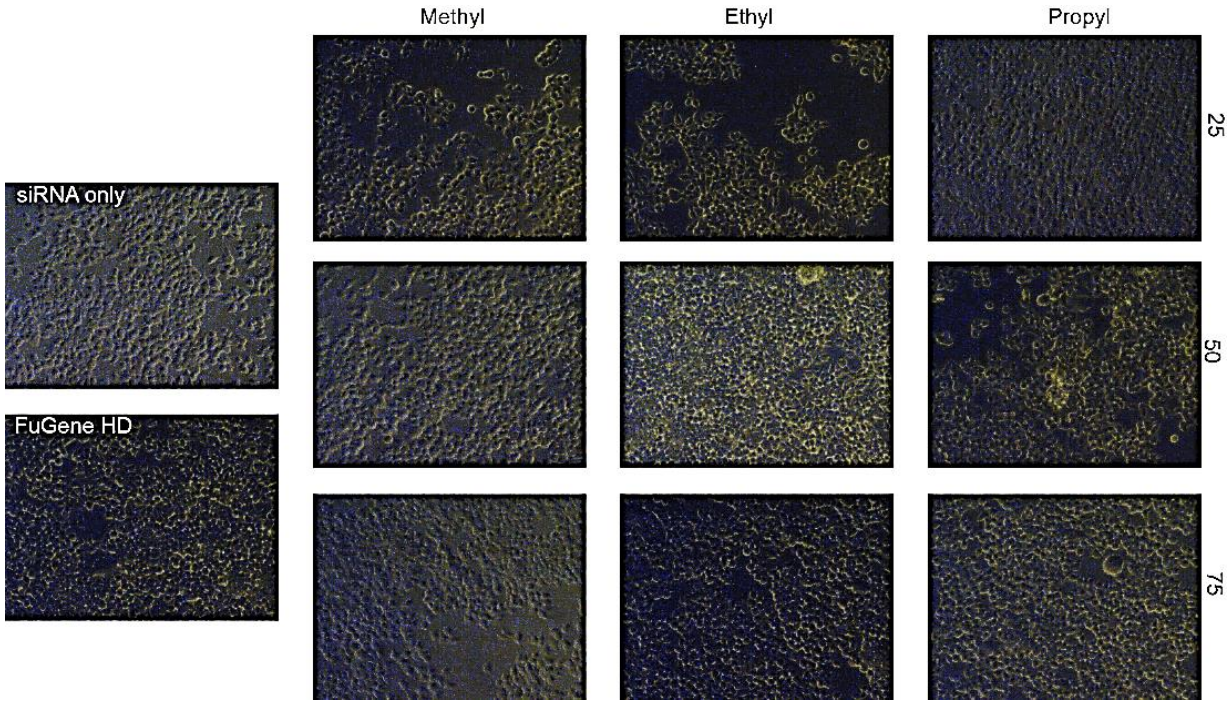

Figure 3.4 *In vitro* study utilizing HEK293 cell line to determine the cellular update ability of the siRNA/copolymer complexes with a fluorescing signal indicating effective gene delivery.

3.4.5 Copolymer Toxicity

In order to evaluate the effect of the tertiary amine functionalities and cationic block length on cell viability, the copolymers were analyzed for their ability to induce an immunogenic response. To investigate these cytotoxic effects, the copolymers were incubated with MCF-7 cells for 48 hours after which time MTS viability assays were utilized for characterization. The resulting cell viability after the subtraction of background absorption and data normalization to the control is shown in Figure 3.5. High levels of cell viability (>90% after 48 hr) were observed for all

copolymers tested with the exception of E50 and E75 which indicate high levels of toxicity (<50% cell viability). Here, the addition of the hydrophilic block did not significantly affect the toxicity levels of E50 and E75 as expected.

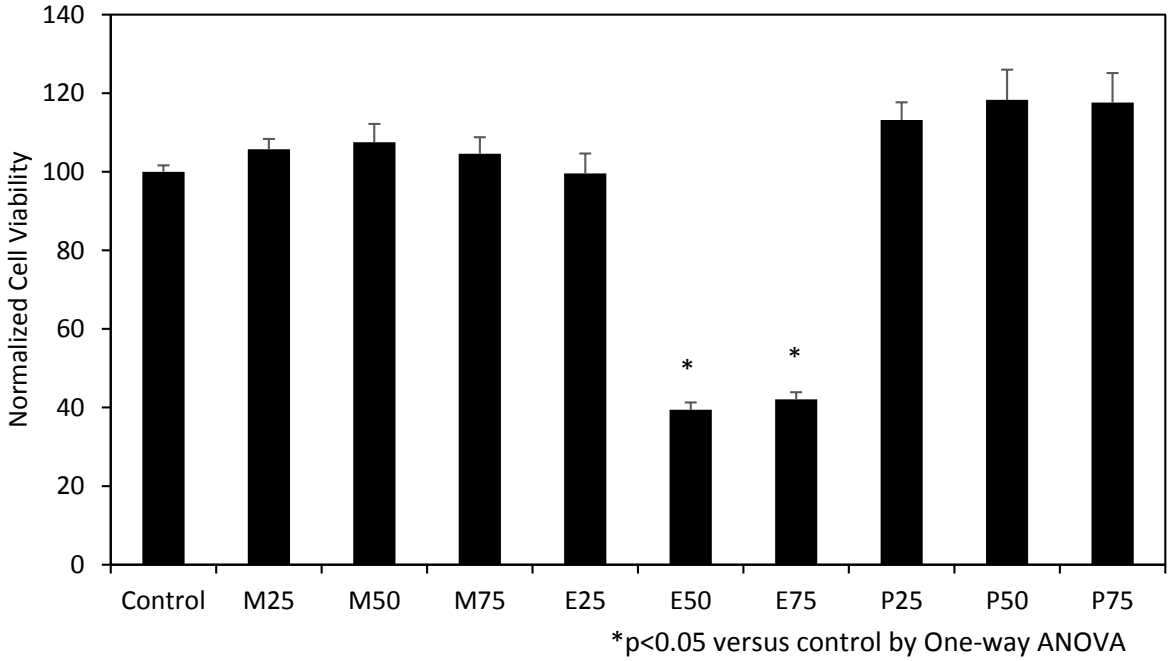

Figure 3.5 Cytotoxicity study of the copolymer series. Most polymers were nontoxic with the exception of E50 and E75 proving to be significantly toxic to the cell line.

3.4.6 Polyplex-Mediated Gene Knockdown

In order to investigate the ability of the copolymers to effectively deliver genetic material to the nucleus, gene knockdown experiments in MCF-7 cells were employed utilizing the polyplex N/P ratio of 3:1. The siRNA/polymer complexes were incubated with the MCF-7 cells for 48 hours. After this time, MYC expression was evaluated and normalized to GAPDH with the resulting data illustrated in Figure 3.5. All polymers with the exception of P75 express a significant decrease in the MYC expression as compared to that of FuGene; therefore, the block polymers indicate potential for successful gene delivery vehicles. Interestingly, there is not an apparent

trend for the different tertiary amine functional groups or degrees of polymerization; however, there are differences among each respective series. Among all polymers, a significant difference in the MYC knockdown is not observed so one block copolymer cannot be named superior over the others studied.

As reported, E50 and E75 induce a toxic response in MCF-7 cells resulting in low cell viability. Though they induce this cytotoxic activity, these two block copolymers are still capable of gene knockdown. This experiment was designed to normalize the inputs as well as the results in order to take cell death into consideration. Normalizations included the cDNA input, the MYC to GAPDH expression, and the polymer treatments to the control. Figure 3.5, therefore, indicates that E50 and E75 are plausible candidates for a viable gene delivery vehicle despite their toxic effect.

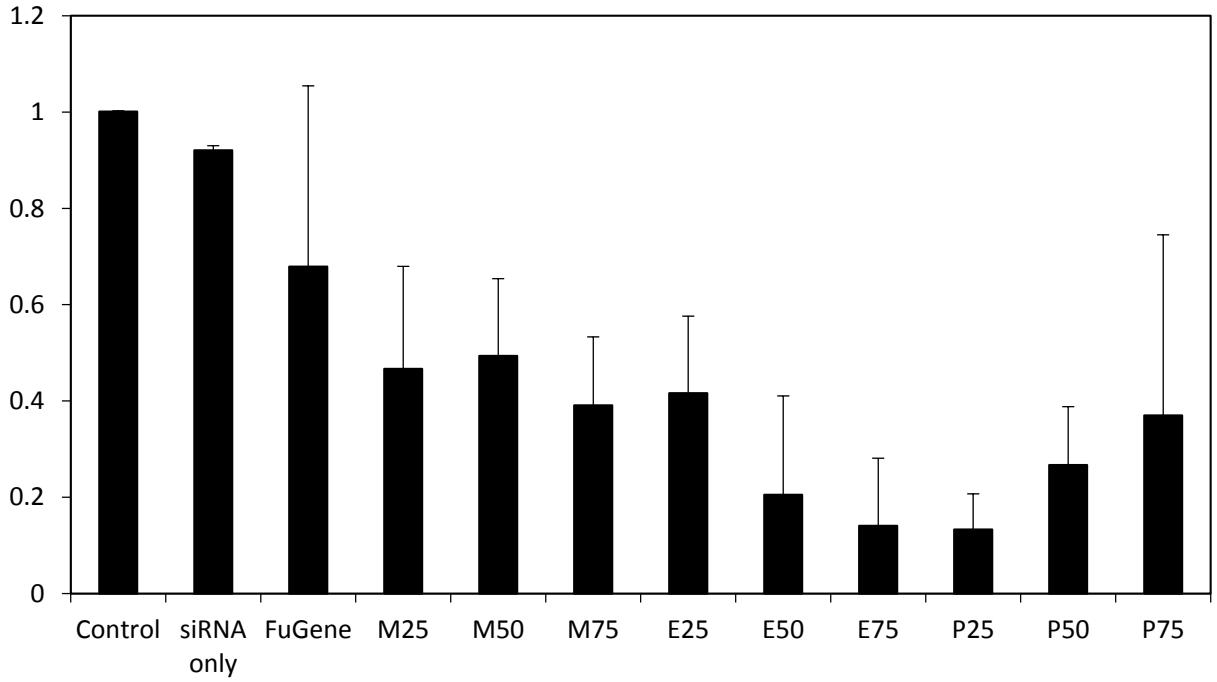

Figure 3.5 qPCR results indicating a significant decrease in the MYC expression for the copolymers as compared to FuGene with the exception of P75.

3.5 Conclusions

The advent of RAFT polymerization offers many advantages to the synthesis of biologically compatible block copolymers in that well-defined molecular weight and architectures are now possible. The use of this polymerization method has brought many advances to the potential use of gene-based therapies in a clinical setting. Here, we have reported on the development of a novel, diblock copolymer series capable of condensing genetic material and escaping the endosome by means of a pH-responsive endosomolytic block. These copolymers were synthesized with a biocompatible A-block composed of OEGMA and a cationic B-block of DMAEMA, DEAEMA, or DPAEMA with the aim to separate out the effects of repeat unit structure and block length of the cationic block on the efficiency of nucleic acid delivery. The results determined from this study indicate a link between cationic block length and repeat unit structure on the gene delivery efficacy. Pairing the low toxicity and effectiveness, this copolymer family will enable further studies and development for promising gene delivery vehicles capable for clinical use.

CHAPTER 4

FUTURE DIRECTIONS

From our studies, we have successfully developed an efficient nucleic acid delivery vehicle that exhibits high cell viability and cell transfection. Moving forward, we hope to further investigate these pH-responsive block copolymers by characterizing their affinity and delivery efficiency of a G-quadruplex (G4) clamp as developed by the research team led by Tracy Brooks. It has been reported that G-quadruplexes appear in the promoter region of the MYC oncogene, and their stabilization leads to downregulation of MYC expression.[39] The G4 clamp is composed of complementary sequences to flank either side of the G-quadruplex of the promoter region held together by a linker sequence. Once this G4 clamp is bound, the quadruplex is stabilized and gene expression decreases. Should the copolymers presented in this study effectively deliver this G-quadruplex clamp, we can stabilize the quadruplex and cease MYC expression.

LIST OF REFERENCES

REFERENCES

(1) Young, R.J.; Lovell, P.A. *Introduction to Polymers Third Edition,* **2011**.

(2) Barner-Kowollik, Christopher. *Handbook of RAFT Polymerization,* **2008.**

(3) Ahmed, M; Narain, R. *Progress in Polymer Science*, **2013**, 38, 767-790.

(4) York, AW; Kirckland, SE; McCormick CL. *Advanced Drug Delivery Reviews*, **2008**, 60, 1018-1036.

(5) Chiefari, J; Chong, YK; Ercole, F; Kristina, J; Jeffery, J; Le TPT; Mayadunne, RTA; Meijs, GF; Moad, CL; Moad, G; Rizzardo, E; Thang, SH. *Macromolecules*, **1998**, 31, 5559-5562.

(6) Le, TP; Moad, G; Rizzardo, E; Thang, SH. WO 9801478 **1998**.

(7) Moad, G; Rizzardo, E; Thang SH. *Australian Journal of Chemistry*, **2005**, 58, 379-410.

(8) Corpart, P; Charmot, D; Zard, S; Franck, X; Bouhadir, G. WO 9935177 **1999**.

(9) Charmot, D; Corpart, P, Adam, H; Zard, SZ; Biadatti, T; Bouhadir, G. *Macromolecular Symposia*, **2000**, 150, 23-32.

(10) Smith, AE; Xu, X; McCormick, CL. *Progress in Polymer Science*, **2010**, 35, 45-93.

(11) Chiefari, J; Mayadunne, RTA; Moad, CL; Moad, G; Rizzardo, E; Postma, A; Thang, SH. *Macromolecules*, **2003**, 36, 2273-2283.

(12) "What is Gene Therapy." *Learn.Genetics Genetic Science Learning Center*. University of Utah Health Sciences. Web. 14 April 2016. <http://learn.genetics.utah.edu/content/genetherapy/gtintro/>

(13) Pack, DW; Hoffman, AS; Pun S; Stayton, PS. *Nature Reviews: Drug Discovery*, **2005**, 4, 581-593.

(14) Wong, SY; Pelet, JM, Putnam, D. *Progress in Polymer Science*, **2007**, 32, 799-837.

(15) Mintzer, MA; Simanek, EE. *Chemical Reviews*, **2009**, 109, 259-302.

(16) Gary, DJ; Puri, N; Won, YY. *Journal of Controlled Release*, **2007**, 121, 64-73.

(17) Varkouhi, AK; Scholte, M; Haisma, HJ. *Journal of Controlled Release*, **2011**, 151, 220-228.

(18) Boussif, O; Lezoualc'H, F; Zanta, MA; Mergnyt, MD; Schermant, D; Demeneix, B; Behr, JP. *Proceedings of the National Academy of Sciences of the United States of America*, **1995**, 92, 7297-7301.

(19) Jones CH; Chen CK; Ravikrishnan A; Rane S; Pfeifer BA. *Molecular Pharmaceutics*, **2013**, 10, 4082-4098.

(20) Werth, S; Urban-Klein, B; Dai, L; Hïbel, S;Grzelinski, M; Bakowsky, U; Czubayko, F; Aigner, A. *Journal of Controlled Release*, **2006**, 112, 257-270.

(21) Grandinetti, G; Ingle, NP, Reineke, TM. *Molecular Pharmaceutics*, **2011**, 8, 1709-1719.

(22) Deshpande, MC; Garnett, C; Vamvakaki, M; Bailey, L; Armes, SP; Stolnik, S. *Journal of Controlled Release*, **2002**, 18, 185-199.

(23) Deshpande, MC; Davies, MC; Garnett, MC; Williams, PM; Armitagea, D; Bailey, L; Varnvakakib, M; Armesb, SP; Stolnika, S. *Journal of Controlled Release*, **2004**, 97, 143-156.

(24) Venkataraman, S; Ong, WL; Ong ZY; Loo, SCJ; Ee, PLR; Yang, YY. *Biomaterials*, **2011**, 32, 2369-2378.

(25) Cherng, JY; van de Wetering, P; Talsma, H; Crommelin, DJA; Hennink, WE. *Pharmaceutical Research*, **1996**, 13, 1038-1042.

(26) van de Wetering, P; Moret, EE, Schuurmans-Niewuwenbroek, NME; van Steenbergen, MJ; Hennink, WE. *Bioconjugate Chemistry*, **1999**, 10, 589-597.

(27) van de Wetering, P; Cherng, JY; Talsma, H; Hennink, WE. *Journal of Controlled Release*, **1997**, 49, 59-69.

(28) Hinton, TM; Guerrero-Sanchez, C; Graham, JE; Le, T; Muir, BW; Shi, S; Tizard MLV; Gunatillake, PA; McLean, KM; Thang, SH. *Biomaterials*, **2012**, 22, 7631-7642.

(29) Manganiello, MJ; Cheng, C; Convertine, AJ; Bryers, JD; Stayton, PS. *Biomaterials*, **2012**, 33, 2301-2309.

(30) Convertine, AJ; Benoit, DSW; Duvall, CL; Hoffman, AS; Stayton, PS. *Journal of Controlled Release*, **2009**, 133, 221-229.

(31) Nelson, CE; Kintzing, JR; Hanna, A; Shannon, JM; Gupta, MK; Duvall, CL. *ACS Nano*, **2013**, 7, 8870-8880.

(32) Liu, Z; Zhang, Z, Zhou, C; Jio, Y. *Progress in Polymer Science*, **2010**, 35, 1144-1162.

(33) Guo, X; Huang, L. *Accounts of Chemical Research*, **2012**, 45, 971-979.

(34) Aied, A; Greiser, U; Pandit, A; Wang, W. *Drug Discovery Today*, **2013**, 18, 1090-1098.

(35) Godbey WT; Barry MA; Saggau P; Wu KK; Mikos AG. *Journal of Biomedical Materials Research Part A*, **2000**, 51, 321-328.

(36) Heath, WH; Senyurt, AF; Layman, J; Long, TE. *Macromolecular Chemistry and Physics*, **2007**, 208, 1243-1249.

(37) Boyer, C; Teo J; Phillips, P; Erlich, RB; Sagnella, S; Sharbeen, G; Dwarte, T; duong, HTT; Goldstein, D; David, TP; Kavallaris, M; McCarroll, J. *Molecular Pharmaceutics*, **2013**, 10, 2435-2444.

(38) "What Affects the Relative Fluorescence of Fluorescein?" Turner Designs. Web. 17 April 2016. <http://www.turnerdesigns.com/what-affects-relative-fluorecence-of-fluorescein>.

(39) Brown, RV; Danford, FL; Gokhale, V; Hurley, LH; Brooks, TA. *The Journal of Biological Chemistry*, **2011**, 286, 41018-41027.

VITA
ANNIE KATHERINE MCCLELLAN

EDUCATION

University of Mississippi *(2013 - Present)* **Oxford, MS**
M.S. Engineering Science, Chemical Engineering Emphasis
NASA/Mississippi Space Grant Consortium Fellow
Anticipated Graduation Date: May 2016 Cumulative GPA: 3.33
Master's Thesis: "RAFT Polymerization of pH-Responsive, Diblock Copolymers for Nucleic Acid Delivery Vehicles"

University of Mississippi *(2008-2013)* **Oxford, MS**
B.S. Chemistry
B.A. Biological Sciences, Mathematics Minor
Graduation date: May 2013 Magna Cum Laude Cumulative GPA: 3.79
Honor's Thesis: "Spectroscopic Study of Charge Transfer Induced Blue Shifting of Pyrimidine/Water Mixtures on Silver Substrate"

WORK EXPERIENCE

ExxonMobil Refining and Supply *(August – December 2015)* **Baytown, TX**
Coordination and Product Quality Department, Profitability Co-op *(Fall 2015)*
- Enhanced SQL and VBA coding skills by incorporating queries and macros into a new Excel tool that acquires and organizes plant simulation data
- Learned to bridge economic and technical considerations to make the most profitable decisions for daily plant operation
- Advanced hazard recognition skills by developing two different safety procedures to be used as safety assessment resources by fellow employees
- Matured leadership qualities as sub-project lead for United Way Day of Caring

ExxonMobil Chemical Company *(January – August 2015)* **Baytown, TX**
Planning and Technology Section, Planning Co-op *(June – August 2015)*
- Gained experience developing project scope for potential capital expenditures
- Determined solution to a new feedstock option with potential to save the plant $7.5M/yr
- Advanced critical thinking and technical skills by solving challenges and determining the most economic course of action for multiple project progressions
- Further developed technical presentation skills by presenting project findings to an audience of piers, supervisors, and managers

Business and Technical Department, Technical Co-op *(January – May 2015)*
- Utilized design practices and technical knowledge to design restriction orifices that increase furnace safety reliability and decrease maintenance costs of operation
- Developed skills in VBA and further refined coding ability by creating a monitoring tool utilizing Excel VBA to pull, organize, and graph plant data
- Introduced to EPA and other environmental agency regulations; utilized these regulations to create a console alarm to reflect permit updates for the site

RESEARCH EXPERIENCE

Graduate Research Assistantship *(2013-2016)* **Oxford, MS**

"RAFT polymerization for the synthesis of tertiary amine-based diblock copolymer nucleic acid delivery vehicles" (to be submitted Spring 2016)

- Developed skills in RAFT polymerization of uniform biopolymers
- Gained experience in gel permeation chromatography (GPC), nuclear magnetic resonance (NMR) spectroscopy, and dynamic light scattering (DLS)
- Became proficient with utilizing electrophoresis and *in vitro* methods to study the binding affinity and gene delivery efficiencies of amphiphilic copolymers
- Responsible for accuracy and maintenance of the GPC
- Conference presentations:
  - 2014 AIChE Annual Meeting
  - 2013 National Graduate Research Polymer Conference

NASA Mississippi Space Grant Consortium Fellow *(2014-2015)* **Oxford, MS**

"Polymer-functionalized graphene nanosheets utilizing RAFT polymerization"

- Assisted a local middle school robotics group on the development of their robot for competition
- Utilized RAFT polymerization to develop graphene functionalized nanomaterials

University of Mississippi Undergraduate Research, *University, MS (June 2010 – May 2013)*

"Surface Enhanced Raman Spectroscopy (SERS) of Pyrimidine Mixtures"

- Introduced to research methods and how to overcome obstacles to see a project to completion
- Learned how to effectively communicate in a technical language as well as how to tailor a presentation for varying audiences
- Developed skills in vapor deposition techniques and accumulating Raman and SERS spectra
- Utilized results of electronic structure computations to verify experimental results
- Conference poster presentations:
  - 245th National ACS Meeting 2013
  - 23rd National NSF EPSCoR Conference 2013
  - 2012 MS EPSCoR Meeting
  - 2011 MS EPSCoR Meeting
  - 242nd National ACS Meeting 2011
  - SWRM/SERMACS 2010

PROFESSIONAL TRAINING

Light Scattering University *Wyatt Technology, Santa Barbara, CA (July 2013)*

- Week long professional training of light scattering analytical equipment
- Participated in light scattering seminars on the principles behind Rayleigh and Raman scattering
- Received highest overall grade of the training class

Diamond Anvil Cell High Pressure Raman Spectroscopy Symposium *(August 2011)*
easyLab Technologies, Ltd. University of Reading, Reading, UK
- Instruction of use and application of a diamond anvil cell for high pressure spectroscopic research

ADDITIONAL INVOLVEMENT

- AIChE Member: 2013 to Present
- United Way Volunteer
- 2016 Bike & Build Rider
- 2014 Graduate Student Council
- Sally McDonnell Barksdale Honors Scholar
- ACS Member: 2010 to Present
- Habitat for Humanity Volunteer
- ExxonMobil Cycling Team
- Church ministry involvement
- 2013 President of Local Student ACS Chapter